Version of Record: https://www.sciencedirect.com/science/article/pii/S0950061820316913
Manuscript_0b2d6d4fc6fd212a658130864355efd7

Effect of fineness and citric acid addition on the hydration of ye'elimite

Y. EL KHESSAIMI [1,2], Y. EL HAFIANE [1], A. SMITH [1]

[1] IRCER, UMR CNRS 7315, Université de Limoges, Centre Européen de la Céramique, 12 avenue Atlantis, 87068 Limoges cedex.

[2] Materials Science and Nano-engineering Department. Mohammed VI Polytechnic University. Lot 660.Hay Moulay Rachid.43150 Ben Guerir. Morocco.

Abstract

The first purpose of this article is to investigate the effect of fineness on the hydration of highly pure ye'elimite powders prepared by solid state reaction or by a chemical route. The second purpose is to examine the role of fineness on the hydration of model calcium sulfoaluminate cements (CSA) prepared by mixing our lab-made ye'elimite with gypsum. The last part concerns the effect of citric acid addition on hydration of a model cement. The main results are the following: (i) ettringite and hydrates formation can be accelerated by the presence of very fine ye'elimite powder in a CSA cement paste; (ii) the hydration rate of CSA model cement depends mainly on the dissolution rate of ye'elimite which can be delayed by the addition of citric acid in water; (iii) the surface of ye'elimite grains presents scarce etch pits when citric acid is present in the water, while the surface seems to be totally attacked with water.

Keywords

Ye'elimite; Fineness; Citric acid; Ettringite; Monosulfoaluminate; Gibssite; Hydration; CSA cement.

Highlights

- Hydration of very fine ye'elimite powder prepared by sol-gel method;
- The influence of ye'elimite fine microstructure on its hydration was studied for the first time;
- The formation of etch-pits during ye'elimite dissolution;

© 2020 published by Elsevier. This manuscript is made available under the CC BY NC user license
https://creativecommons.org/licenses/by-nc/4.0/

- Ye'elimite dissolution governs the hydration rate of CSA model cement;
- Citric acid delays the dissolution of ye'elimite grains;
- Ettringite formation can be accelerated by the addition of highly fine ye'elimite powder;
- Ettringite formation can be delayed by the addition of citric acid.

1. Introduction

For their shrinkage compensation and self-stressing properties, Calcium Sulfoaluminate Cements (CSA) have been developed and produced in China since the last forty years [1]. More recently, the interest of the international cement research community towards these cements comes not only from their expansive behaviour [2], but also from their environmentally friendly characteristics associated to their production, which includes a reduced CO_2 footprint. However, many barriers prevent more widespread usage of this material. Despite having been used in construction for many years [3] relatively little is known about effective mixture design methodology for using CSA cement in concrete infrastructure. In the absence of formalized design guidance, CSA cements are most commonly used in small-scale repairs, where their ability to set rapidly can be advantageous and long working times are not necessary. For larger scale placements, retardation of the CSA reactions is necessary, and citric acid is currently the primary set retarding carboxylic acid recommended for use with CSA cements. However, the mechanism by which citric acid solutions modify the hydration of CSA cements is still not fully understood. Effect of citric acid addition on CSA cement hydration has been well recognized, and studied by several researchers, most of the studies were either based on qualitative description of hydration curves or parameters that indirectly refer to hydration, such as set time and strength [4–7]. Organic compounds like sugars or citric, tartaric or gluconic acids and their salts are powerful retarders in CSA cements [7]. Citrate and tartrate ions are chelating agents of Ca^{2+} and Al^{3+} and would be expected to influence the nucleation and growth of phases containing these ions [8]. Most carboxylic acids have no effect on the morphology of ettringite crystals. This probably results from the fact that the calcium ions of the crystals are buried in a sheet of negatively charged hydroxyl and water molecules and the negatively charged carboxylate groups are repelled by

51 the negatively charged crystals [8]. The mechanism through which citric acid influences the
52 hydration kinetics of the CSA systems is not fully understood. However, researchers have found that
53 citrate will form chelates with calcium on the surface of a cement, thus hindering cement dissolution,
54 in addition to forming chelates with calcium ions already in solution and reducing their availability
55 for participation in hydration reactions [9]. Another inorganic retarder acid applied for CSA-type
56 cements is boric acid, it inhibits the nucleation of ettringite, but instead it allows six-sided plates of
57 the metastable monosulfoaluminate phase to form [8,10].
58 The first authors who worked on the influence of citric acid on hydration reactions in the
59 $3CaO.Al_2O_3$-$CaSO_4.2H_2O$-CaO-H_2O system were Tinnea and Young [5]. They found that hydration
60 reactions are retarded by the addition of citric acid. Ettringite and monosulfoaluminate were all
61 detected as early hydration products. The influence of citric acid as a retarder for ternary binders
62 based on Ordinary Portland Cements (OPC), CSA and anhydrite was investigated by Winnefeld et
63 al. [6]. Their main conclusions were that the addition of citric acid retarded the early ettringite
64 formation, lengthened the workability time, and reduced significantly the compressive strength even
65 after 28 days. Zhang et al. [11] studied the effect of citric acid on the fluidity and strength of CSA
66 commercial cements. They found that the initial fluidity of paste admixed with superplasticizers
67 would be decreased by the presence of citric acid. Moreover, both early and late strengths of cement
68 were decreased by the addition of citric acid. In a recent study about the effect of citric acid on
69 hydration properties of commercial CSA, Burris et al. [4] found that citric acid successfully retarded
70 initial set by 120 min for CSA cement. Despite the reported studies about the effect of citric acid on
71 CSA cements hydration, there is a lack of understanding about how changing retarder dosage
72 influences cement hydrates formation. It represents a serious barrier to specification and, in
73 particular, larger scale usage of CSA cements.
74 From a materials scientist point of view, one parameter which dictates the reactivity of a powder
75 (with water for instance, or during sintering) is its fineness. Cement fineness is considered as one of
76 the major variables influencing cement properties and concrete strength [12–15]. It is also a
77 dominant factor that affects cement hydration since the fineness directly controls the volume of

78 water available for hydration for each unit volume of cement particle, as well as the inter-particle
79 spacing between them [16]. The aim of nanoparticle addition in cements is the stimulation of
80 nucleation processes during the early cement hydration. The earlier these nuclei are formed, the
81 earlier they can grow to larger crystals of hydration phases and thereby accelerate the cement
82 hydration [17].
83 In the literature on cementitious materials and specifically Portland cements, different authors
84 mentioned the effect of fineness on hydration [12,18–22]. Thomas [19] examined the hydration of
85 the β polymorph of belite (calcium di-silicate). He observed that if this polymorph had a specific
86 surface area similar to a Portland cement, it was less reactive with water than a β-belite prepared by a
87 chemical route (Pechini process). Pollman [20] and Hong [21] indicated that the interest in using
88 chemical synthesis methods was to be able to study the hydration behaviour of pure belite and in
89 particular fine particles. The interplay between fineness and chemical composition of fillers
90 (limestone, alumina, silica) on Portland mortars hydration was studied by Kadri et al. [13]. Whatever
91 the type of filler, the finer it is, the more accelerated the early hydration of the mortar is. Fineness
92 can also influence Portland concrete properties such as self-compaction, shrinkage, durability or
93 reduction of product cost. A study is needed to accurately interpret the hydration process and
94 quantify effects of cement fineness on CSA cement hydration and the role of ye'elimite fineness on
95 hydration has not been studied.
96 Cement hydration is a complex process, because cement powder contains several inorganic phases.
97 A simple way to well investigate the effect, is to examine the hydration of the main reactive
98 cementitious phase in different controlled hydration conditions. CSA cements can have highly
99 variable compositions, but all of them contain the key-phase ye'elimite, $Ca_4(AlO_2)_6SO_4$ (noted
100 $C_4A_3\overline{S}$ in cementitious notation) [23–25].
101 In fact, ye'elimite hydration proceeds through dissolution and precipitation [26], leading to the
102 precipitation of various hydrates. In the presence of anhydrite (calcium sulfate, $CaSO_4$ or $C\overline{S}$),

ye'elimite hydrates to form ettringite $Ca_6Al_2(SO_4)_3(OH)_{12}.26H_2O$ or ($C_6A\overline{S}_3H_{32}$*) as well as gibbsite $Al(OH)_3$ or (AH_3) (Reaction 1) [2,27–29]:

$$C_4A_3\overline{S} + 2\,C\overline{S} + 38\,H \rightarrow C_6A\overline{S}_3H_{32} + 2\,AH_3 \quad (R1)$$

Ye'elimite — Anhydrite — Water — Ettringite — Gibbsite

In the absence of calcium sulfate, the hydration of ye'elimite can lead to the formation of monosulfoaluminate ($Ca_4Al_2(SO_4)(OH)_{12}.6H_2O$ or $C_4A\overline{S}H_{12}$) and gibbsite (Reaction 2) [2,27–29]:

$$C_4A_3\overline{S} + 38\,H \rightarrow C_4A\overline{S}H_{12} + 2\,AH_3 \quad (R2)$$

Ye'elimite — Water — Monosulfoaluminate — Gibbsite

Recently, significant work has been carried out on ye'elimite single phase hydration, pioneered by Hanic et al. [30]. Ye'elimite hydration was shown to occur through a two-step reaction. The reaction product in the first step was ettringite, whereas monosulfoaluminate $C_4A\overline{S}H_{12}$ was the hydration product in the second step of hydration reaction. Suspensions of synthetic ye'elimite in a saturated gypsum solution were also investigated [31]. The most voluminous hydration product observed was ettringite. During the hydration of orthorhombic ye'elimite in dilute suspensions with a water over binder mass ratio equal to 40 and 100, Bullerjahn et al. [32] identified five stages of hydration: stage I (initial period), stage II (dormant period), stage III (acceleration period), stage IV (main hydration period) and stage V (final period). The duration of each stage was directly linked to the evolution of the solution concentrations and the type of hydration reaction [33]. Other authors were interested in the hydration behavior of orthorhombic and pseudo-cubic ye'elimite [34–36]. It was shown that in the absence of additional sulfate sources, orthorhombic-ye'elimite reacts slower than pseudo-cubic-ye'elimite, and monosulfoaluminate phases are the main hydrated crystalline phases (see reaction R2). However, in the presence of additional sulfates, orthorhombic-ye'elimite reacts faster than pseudo-cubic-ye'elimite, and the main hydrated crystalline phase is ettringite (see reaction R1). The published data on ye'elimite single phase hydration [34–37] are summarized in Fig. 1, which shows

*The cement phase notations are used in this work (C = CaO, A = Al_2O_3, $\overline{S}$ = SO_3, $\overline{C}$ = CO_2, H = H_2O)

the degree of ye'elimite hydration (α) (Fig. 1a) and the amount of the formed hydrates (Figs 1b, 1c and 1d). The degree of ye'elimite hydration, α, is calculated as follows:

$$\alpha(\%) = \frac{\mathrm{wt\%^{ye'elimite}}(t_0) - \mathrm{wt\%^{ye'elimite}}(t)}{\mathrm{wt\%^{ye'elimite}}(t_0)} \times 100 \quad \text{(E.1)}$$

where ($\mathrm{wt\%^{ye'elimite}}$) refers to the weight percentage of ye'elimite, (t_0) is the starting hydration time and (t) is the final hydration time, the hydration duration corresponds to ($t-t_0$). The amounts of formed hydrates (see Figs. 1b to 1d), namely ettringite, monosulfoaluminate and gibbsite, are directly extracted from the literature data. The plots show that depending on the authors, a large range of hydration degrees, α, can be found in the literature. Besides, ye'elimite hydration degree influences upon the amount of the formed hydrates, especially ettringite, and it depends on parameters, such as the presence of minor elements (iron, sodium) and the initial water over cement mass ratio. Thereby, physical and chemical characteristics of ye'elimite play a significant role on CSA hydrates formation. The study of ye'elimite hydration under controlled conditions of fineness and citric acid dosages can contribute to better understand the link between these two parameters and CSA cement hydration.

In this context, this paper tends to clarify the effect of these two factors, namely fineness and citric acid addition, on the hydration of ye'elimite-rich cements. It can contribute to a better understanding of the early age expansion of industrial expansive CSA [38]. The paper starts by discussing the effect of fineness and citric acid addition on the dissolution of pure ye'elimite powder prepared by solid state reaction or by a chemical route; for the first part of the work, the pure ye'elimite powder is in dilute suspensions. Then, in a second part of the work, model CSA cements are prepared by mixing pure ye'elimite with gypsum. In order to prepare cement pastes, these model cements are mixed with water alone or water containing citric acid. The aim is to examine how citric acid can influence the hydration kinetics and the chemical nature of the hydrated products. The studied CSA model systems show a schematic picture of the early behaviour of commercial CSA cements [38]. Despite the fact

148 that model cements do not reflect the whole complexity of commercial products, it helps to give a
149 basic understanding of the hydration by focussing on the major hydration reactions [38].
150 The experimental approach of the present study focuses on identifying the nature and the amount of
151 the hydration products using Rietveld analysis coupled to TGA analysis and on monitoring the
152 ye'elimite dissolution using continuous ionic conductivity measurement. Zeta potential
153 measurements were also carried out to examine the mechanisms by which citric acid acts on
154 ye'elimite-rich cement hydration.

155 2. Materials and methods

156 2.1. Materials

157 Ye'elimite $C_4A_3\overline{S}$ powder was synthesized by solid state reactions from a 4:3:1 stoichiometric
158 mixture of calcium carbonate ($CaCO_3$, CAS number: 471-34-1, Sigma-Aldrich, >99.9 wt.%),
159 alumina (Al_2O_3, CAS number: 1344-28-1, Acros-Organics, >99.7 wt.%) and highly pure gypsum
160 ($CaSO_4.2H_2O$, CAS number: 10101-41-4, Sigma-Aldrich, >99.0 wt.%) powder. The raw materials
161 were dry homogenized. The homogenized powders were then pressed into pellets (20 mm in
162 diameter) and heated at 1300°C for 3 h. After 3 h, the samples were quenched in air. The pellets
163 were reground with an excess of anhydrite in order to compensate sulfate volatilization during
164 thermal treatment and then the powder was pressed again into disks before further heating. The
165 pellets were quenched in air after this last heating and finally ground with an agate mortar. A
166 detailed description about the synthesis protocol can be found in [25]. The sample was labelled: **Ye-**
167 **sol**.

168 Ye'elimite was also synthesised by sol-gel method using the Organic Steric Entrapment route (OSE).
169 A stoichiometric mixture of three salts ($Ca(NO_3)_2.4H_2O$, CAS number: 13477-34-4, Fisher
170 Scientific, >99.0 wt.%), ($Al(NO_3)_2.9H_2O$, CAS number: 7784-27-2, Fisher Scientific, >99.0 wt.%),
171 and ($Al_2(SO_4)_3.16H_2O$, CAS number: 17927-65-0, Fisher Scientific, >98.0 wt.%) was added to a 5
172 wt.% aqueous solution of (PVA, CAS number: 9002-89-5, VWR Chemicals). The resulting gel was

dried, then finely ground and finally calcined at 1250°C for 1 h. More details about the synthesis protocol can be found in [39]. The sample was labelled: **Ye-chem**.

Since ye'elimite hydration depends on $C_4A_3\overline{S}$ polymorphs [34,35], only orthorhombic ye'elimite powders were synthesised to minimize parameters affecting hydration. In this respect, Ye-sol and Ye-chem refer to orthorhombic ye'elimite phase. The synthesised ye'elimite powders were found highly pure, with the presence of some impurities such as CA and CA_2. In other works, C_3A and $C_{12}A_7$ were detected as impurities [25,39–41]. The presence of calcium aluminate impurities depends on the kinetic of solid state reactions during ye'elimite formation. It was shown that the kinetic depends mainly on alumina grain size used as a raw material for ye'elimite lab-synthesis [42].

To prepare a CSA model cement, Ye-sol was blended with gypsum $CaSO_4.2H_2O$ ($C\overline{S}H_2$ in cementitious notation) (CAS number: 10101-41-4, Sigma-Aldrich, > 99.0 wt.%). In order to examine the effect of citric acid on ye'elimite hydration, commercial citric acid ($HOC(CH_2CO_2H)_2CO_2H$, CAS number: 77-92-9, Sigma-Aldrich) was used.

The different samples and the corresponding characterization techniques are summarized in Table 1.

2.2. Characterisation methods

2.2.1. XRD-Quantitative Rietveld analysis

X-Ray Diffraction (XRD) data were collected at room temperature in the Bragg-Brentano geometry using a Bruker D8 Advance X-ray diffractometer with CuKα radiation (λCu = 1.54056 Å, without monochromator; operating voltage of 40 kV and electric current 40 mA). The step scan was 0.02° with a time counting per step of 0.45 seconds. The sample was rotated during data collection at 15 rpm in order to increase particle statistics. The diffractometer was equipped with an energy-dispersive LYNXEYE XE-T detector for filtration of fluorescence and K_β radiation. Mineral phases of the synthesised samples were quantified by using the Rietveld method as implemented in the TOPAS 4.2 software. The fitting parameters were the background coefficients, the phase scales, the zero-shift error, the cell parameters, and the phase shape parameters. The peak shapes were fitted using the pseudo-Voigt function. The Rietveld refinement strategy and the criteria for selecting the

best crystal structure data were based on the recent methods concerning diffraction and crystallography applied to anhydrous cements published by De la Torre et al. [43]. The structures used for fitting the crystalline phases and the respective ICSD (Inorganic Crystal Structure Database) codes [44–48] are given in Table 2. To check the Rietveld fitting quality between measured and calculated diffractograms, reliability factors should be given as, Rwp (weighted profile R-factor), Rexp (expected R-factor) and GOF (Goodness Of Fit) [49]. These reliability factors reflect the deviation between measured intensities (I_{iM}) and calculated intensities (I_{iC}) at any given measurement point (i) as follows:

$$Rwp = \sqrt{\frac{\sum_i w_i(I_{iM}-I_{iC})^2}{\sum_i w_i(I_{iM})^2}} \quad (E.2)$$

$$Rexp = \sqrt{\frac{N-P}{\sum_i w_i(I_{iM})^2}} \quad (E.3)$$

$$GOF = \left(\frac{Rwp}{Rexp}\right)^2 \quad (E.4)$$

where w_i is the attributed weight, N is the number of data points and P is the number of the refined parameters.

Most of AH_3 gel produced during CSA hydration (see reaction R1) is an amorphous phase [50]. In the present paper only crystalline gibbsite was quantified by XRD-Rietveld analysis. Since cement pastes and set cements contain a complex mix of different crystalline and amorphous hydrates, an accurate quantification by Rietveld analysis is sometimes difficult [51,52]. Therefore, our data are considered to be semi-quantitative and absolutely not quantitative.

2.2.2. Scanning Electron Microscopy (SEM)

The prepared samples were examined with a LEO 1530 VP field emission scanning electron microscopy (SEM) equipped with an Energy Dispersive X-ray Spectroscopy (EDS) detector (Oxford INCA 250). The microscope was operated at a 1 kV accelerating voltage. This low voltage is necessary in order to avoid spoiling the sample. The samples were stored in desiccators filled with

219 silica gel prior to and after examination in order to prevent hydration or carbonation. SEM
220 observations were carried out without using a deposited conducting layer. For ye'elimite dissolution
221 experiments, ye'elimite powder was stirred with demineralized water at 500 rpm using a magnetic
222 agitator for the desired time. Hydration was stopped by the solvent exchange method using acetone,
223 then filtered by vacuum aspiration and the samples could then be observed under the SEM.

224 ### 2.2.2. Particle size distribution (PSD) and BET specific surface area (SSA)

225 The PSD was measured in ethanol suspension using Horiba Partica LA-950-V2® applying the
226 Fraunhofer model. Refractive indices of 1.568 and 1.525 were used for ye'elimite $C_4A_3\overline{S}$ and
227 gypsum $C\overline{S}H_2$, respectively [31]. The SSA was estimated from N_2 adsorption/desorption isotherm
228 experiments using a Micromeritics model Asap® 2020 analyzer. Prior to measurements, a degassing
229 step of the sample powder was carried out under vacuum at 110°C during 24 h.

230 ### 2.2.3. Thermogravimetry (TGA)

231 TGA was carried out in N_2 atmosphere on 30 mg of sample using a SETARAM Labsys TG-
232 DTA/DSC thermal analyser at 10 °C/min up to 1100°C.

233 ### 2.2.4. Continuous ionic conductivity measurement (IC)

234 The ionic conductivity measurements with time of ye'elimite suspensions were performed using a
235 CDM210 Conductivity Meter. The water over ye'elimite weight ratio, W/C, is equal to 1000 (Fig. 2).
236 This high dilution has been chosen to avoid the formation of hydrates and in order to have
237 specifically information about ye'elimite dissolution. During the measurement, the suspension was
238 stirred at 500 rpm. The volume of the measurement cell is about 150 ml. The temperature was
239 controlled by a thermostatic bath with external water circulation at 25 °C. Similar experiments were
240 carried out with gypsum alone.

241 ### 2.2.5. Zeta potential measurement (ZP)

242 The interaction between the added citric acid and ye'elimite powder was evaluated by measuring the
243 zeta potential of ye'elimite particles as a function of the citric acid concentration. Suspensions of 0.1
244 wt.% were prepared by mixing for 24 h ye'elimite powder with deionized water containing different

dosages of citric acid (0 wt.%, 5 wt.% and 10 wt.% relative to the weight of ye'elimite powder). The zeta potential was measured using a Malvern ZetaSizer Nano ZS, which is based on the electrophoresis method.

Zeta potential values depend on pH value of the measured suspension. In the present experiments, when 0 wt.%, 5 wt.% and 10 wt.% of citric acid were added, the pH values of the corresponding suspensions were 11.79, 10.84 and 10.80. Therefore, pH values do not vary greatly with the addition of citric acid and the measured Zeta potential values are considered to be taken at pH from 10.8 to 11.79.

2.3. Experimental protocols

Fig. 2 and Fig. 3 summarize the experimental protocols relevant to the preparation and the characterisation of the prepared suspensions and cement pastes.

2.3.1. Preparation of suspensions for ye'elimite dissolution experiments (Fig. 2)

To gain information on the effect of ye'elimite grain fineness on the dissolution kinetics, two suspensions were compared; the first one contained ye'elimite powder synthesised by solid state reactions (**Ye-sol**), and the second one contained ye'elimite powder synthesised by sol-gel method (**Ye-chem**). All suspensions were made by adding the ye'elimite powder to the demineralized water with a water over ye'elimite weight ratio, W/C, equal to 1000. The suspension was stirred at 500 rpm. To examine the influence of citric acid on ye'elimite dissolution, three different concentrations of citric acid were first dissolved in the demineralized water prior to mixing with the powder. The quantities of citric acid were equal to 0 wt.%, 5 wt.% and 10 wt.% relative to the weight of ye'elimite powder; they are labelled **Ye-Sol-0**, **Ye-Sol-5** and **Ye-Sol-10**, respectively. The chosen citric acid dosages are much higher than the common concentration ranges generally used to delay CSA hydration [4,7,11,53,54]. These dosages were chosen in order to allow us to highlight clearly the effect of citric acid addition on hydration.

2.3.2. CSA model cements pastes preparation (Fig. 3)

CSA model cements were prepared by dry mixing gypsum with ye'elimite powder either synthesised by solid state reaction (labelled: **CSA-sol**) or synthesised by sol-gel method (labelled: **CSA-chem**). The cement powders were prepared with a ye'elimite to gypsum weight ratio, (Ye/Gy) of 2. The hydration was studied on cement pastes with a water to cement (cement = Ye + Gy) weight ratio, W/C of 2. Performing the hydration study at these chosen Ye/Gy and W/C ratios should allow full ettringite precipitation [27]. The pastes were mixed, sealed in polyethylene containers and stored at 20°C for 3 days, 7 days and 28 days. These durations correspond to typical storage conditions for testing various properties of set cements (EN 196-1 [55]).

To study the influence of citric acid on the hydration of CSA model cement, three different concentrations of citric acid were pre-dissolved in the mixing water, equivalent to 0 wt.%, 0.5 wt.% and 1 wt.% relative to ye'elimite powder weight, labelled **CSA-sol-0**, **CSA-sol-0.5** and **CSA-sol-1**, respectively. The chosen citric acid dosages are within the common concentration ranges generally used to retard CSA cements [4,7,11,53,54]. After completion of the expected hydration durations, the hydration process was stopped, and samples were kept in a dry atmosphere (desiccator filled with silica gel) until analysis.

2.3.3. Hydration stoppage method

The solvent exchange method was used to stop the hydration of the hydrated pastes. To this end, the hydrated paste was smoothly ground in an agate mortar and then mixed in 150 ml of acetone for 6 min. Afterwards, the liquid was filtered from the sample by vacuum filtration.

3. Results and discussion

3.1. PSD and BET of ye'elimite and gypsum

In our previous works concerning ye'elimite synthesis [25,39], the mineralogical composition determined by XRD-quantitative Rietveld analysis, particle size distribution (PSD), powder microstructure and BET specific surface area (SSA) of the two-synthesised ye'elimite powders were studied (Table 3). The micrographs and the BET data show that Ye-chem powder presents a smaller average grain size (136 nm) and a higher specific surface area (2.2 m^2/g), in comparison to Ye-sol

296 powder, which has (2 µm) and (0.74 m^2/g) as average grain size and specific surface area,
297 respectively. On the contrary, the particle size distribution measured by laser diffraction reveals
298 higher D_{50} for Ye-chem powder (27.1 µm) than for Ye-sol (14.6 µm). This is due to the
299 agglomeration state of Ye-chem powder as shown in SEM micrographs in Table 3.

300 In order to prepare the CSA model cements, highly pure gypsum (> 99.0 wt.%) was used. It has the
301 following characteristics: 4.19 m^2/g as BET surface area, and particle size diameters equal to d_{10} =
302 9.92 µm, d_{50} = 23.08 µm and d_{90} = 45.32 µm.

303 ### 3.2. Effect of fineness and citric acid on ye'elimite dissolution

304 The dissolution rate of anhydrous cementitious phases is proportional to the slope of the ionic
305 conductivity versus time curves during the first minutes of dissolution. Fig. 4a shows the ionic
306 conductivity variations of the Ye-sol-0, Ye-sol-5, Ye-sol-10 and Ye-chem suspensions (W/C=1000).
307 Provided the temperature remains constant, the ionic conductivity in these highly dilute situations
308 depends mainly on two factors: concentration of ions and ionic mobility. In the present situation, as
309 soon as the powder is in contact with water, dissolution of ye'elimite grains starts and the ions go
310 into solution. Since the concentration of ions starts increasing, the ionic conductivity also increases
311 immediately. It reaches a plateau with Ye-chem after 25 min. The slope value (s) of the different
312 ionic conductivity curves (Fig. 4a) during the first minutes of dissolution (~ 5 min) are in the
313 following order: s (Ye-chem-0) > s (Ye-sol-0) > s (Ye-sol-5) > s (Ye-sol-10). In this later case, it
314 looks as if there is no dissolution within 50 min since the ionic conductivity level remains constant.
315 Thus, the corresponding dissolution rates (r) follow the following sequence as well: r (Ye-chem-0) >
316 r (Ye-sol-0) > r (Ye-sol-5) > r (Ye-sol-10) ≈ 0. Referring to similar conductivity measurements on
317 gypsum suspensions with different citric acid content, respectively 0 wt.% (Gy-0), 5 wt.% (Gy-5)
318 and 10 wt.% (Gy-10) (Fig. 4b), it seems that citric acid does not delay gypsum dissolution kinetics.
319 The slope value of the different ionic conductivity curves (Fig. 4b) during the first minutes of
320 dissolution (~ 5 min) are almost equal. This means that citric acid does not delay gypsum dissolution
321 kinetic and only influences upon ye'elimite dissolution.

To investigate the morphological aspect of ye'elimite grains at early age dissolution stage, SEM micrographs of Ye-chem (Ye-chem-0) and that of Ye-sol powder immersed during 1 min in deionised water (Ye-sol-0), or in 10 wt.% citric acid solution (Ye-sol-10) are shown in Fig. 5. The water to ye'elimite ratio was 1000. After only 1 min, ye'elimite grains immersed in deionised water (Ye-sol-0, Fig. 5a, and Ye-chem-0, Fig. 5c) show a severely corroded surface with the formation of several etch-pits (holes on the micrographs). In the case of ye'elimite which has been in contact with a citric acid solution (Ye-sol-10, Fig. 5b), the ye'elimite grains surface appears smooth and much less attacked; moreover, the scarce etch-pits present characteristic geometries of crystal dissolution [56]. The SEM observations are in agreement with the (IC) measurements and confirm that the chemical nature of the solution in contact with ye'elimite plays an important role on its dissolution. The formation of etch-pits during mineral dissolution has been evidenced in the literature for other cementitious anhydrous phases such as alite (tricalcium silicate, C_3S) and belite (dicalcium silicate, C_2S) [56–59] and other silicates like quartz [60–62]. In fact, the formation of such etch-pits was previously observed on the surface of alite phase grains, the major phase in ordinary Portland cements, by Juilland et al. [56], who stated that etch-pits formation depends on the over/under saturation state of solution, and also on the crystallographic defects density of anhydrous alite grains. Nicoleau et al. [58] confirmed the discussions of Juilland et al. [56] concerning etch-pits formation during alite dissolution, by measuring the dissolution rate of alite according to the solution saturation state. The notion of etch-pits formation during mineral dissolution was identified and theorised early by Lasaga et al. [63] and Burch et al. [64] who observed etch-pits formation during dissolution experiments of quartz and calcium carbonates.

The rapid reactivity of ye'elimite powder synthesised by sol-gel method (Ye-chem) during the early dissolution step could be explained by its microstructure. In fact, Ye-chem powder shows very small ye'elimite grains (136 ±48 nm, Table 3) compared to Ye-sol powder which contains relatively larger ye'elimite grains (2 ±1.2 µm, Table 3). This morphological difference provides ye'elimite surfaces with different reactivity to water.

To highlight the interaction between the added citric acid and ye'elimite powder, zeta potential measurements were carried out on the ye'elimite suspensions, Ye-sol-0, Ye-sol-5 and Ye-sol-10. The pH values of the corresponding acidic suspensions were 11.79, 10.84 and 10.80, respectively. Citric acid is normally considered to be a tri acid, with pKa values at 25 °C, extrapolated to zero ionic strength, of 2.92, 4.28, and 5.21 [65]. Thereby, citrate is the dominant form of citric acid present in our suspensions. The results of zeta potential measurements are shown in Table 4. An increase in the citric acid concentration from 0 to 5 wt. % leads to a shift of the zeta potential from 7.7 ± 0.3 mV to -0.2 ± 0.1 mV, and the zeta potential turns to lower negative values (-10.9 ± 2.8 mV) for Ye-sol-10. The adsorption of citrate molecules at the surface of ye'elimite grains could explain this change of zeta potential values. In citrate, the distances between two oxygen atoms in two neighbouring carboxylate groups, are between 2.7 and 4.0 Å (Fig. 6a) [66]. For ye'elimite, the $(13\bar{1})$ plane is a possible face for a ye'elimite crystal [67]; the distances between two calcium atoms are between 3.0 and 4.0 Å (Fig. 6b). Therefore, the citrate molecules can adsorb on the $(13\bar{1})$ faces via the oxygen of the carboxylate groups to form a chelate. The remaining carboxylate functions of the adsorbed citrate molecules are negatively charged and can be responsible for the negative values of the zeta potential. This citrate adsorption can inhibit ye'elimite grains dissolution. In solution, calcium and citrate can form chelates too [68]. Consequently, two events can explain the slow setting of cement paste containing ye'elimite: the adsorption of citrate at the surface of ye'elimite grains can delay ye'elimite dissolution, and the formation of chelates between calcium and citrate in the solution can prevents calcium ions to participate in hydrates formation. The concept of citrate adsorption on gypsum crystals was adopted by different authors [68–70] to the explain the retarding effect on plaster crystallisation.

Another possible way to explain the effect of citric acid addition in the shifting of the zeta potential from positive values to negative values, is to use Bombled's approach [71]. This author estimated the surface charge of alite (C_3S) particles, and he showed that there are three times fewer positive sites than negative sites. Similarly, Smith et al. [72] applied Bombled's approach to estimate the surface charge of krotite particles (calcium aluminate, CA) and they found that the negative sites are

dominant. The approach is based on a statistical representation of the charges on the surface of grains. It can be expressed as follows:

$$\frac{\sigma^+}{\sigma^-} \text{ is proportional to } \frac{\sum_{\text{positive ions}} r_+^{\,2}}{\sum_{\text{negative ions}} r_-^{\,2}} \qquad \text{(E.5)}$$

where $\frac{\sigma^+}{\sigma^-}$ is the positive to negative surface charge ratio, r_+ is the ionic radius associated to positive ions and r_- is the ionic radius associated to negative ions.

The application of this approach to ye'elimite starts by knowing the ionic radius of each element: 1.35 Å for oxygen, 1.05 Å for calcium, 0.5 Å for aluminium and 0.43 Å for sulphur. $\frac{\sigma^+}{\sigma^-}$ can be calculated and it is proportional to 0.2. This means that the negative sites are dominant and that the surface of the anhydrous $C_4A_3\overline{S}$ ($Ca_4Al_6O_{16}S$) particles is consequently negatively charged. Assuming that all of the calcium ions of the surface form chelates molecules when citrate is present, the $\frac{\sigma^+}{\sigma^-}$ ratio becomes equal to 0.05. This means that negative sites become more dominant. Since zeta potential of a cement suspension is proportional to the surface charge of the cement grains present in this solution [72], the shift of (ζ) from positive to negative values could be explained by the high dominance of negative sites in the $C_4A_3\overline{S}$ particle surface in contact with citrate. Even though Bombled's approach is somewhat simplistic because it assumes that all the surfaces have the same atomic arrangement and that the surface of the grains has the same chemical composition as the bulk, it gives an interesting insight into the variations of the surface charge with the addition of citric acid.

3.3. Hydration of CSA model cements containing ye'elimite with two different grain sizes

The results of XRD analysis of the hydrated CSA model cements CSA-sol and CSA-chem at $t_0 = 0$ day, and after curing for 3 days, 7 days and 28 days are shown in Fig. 7a. The corresponding Rietveld analysis results are given in Table 5. Since we consider that Rietveld analysis gives an approximate picture of the quantities of remaining reactants (ye'elimite and gypsum) and formed hydrates, we will focus for clarity on the amount of remaining ye'elimite and on the total quantities

of formed hydrates (ettringite, the most abundant hydrate, monosulfoaluminate and gibbsite). The nature of the formed hydrate phases is in accordance with experimental results previously published about ye'elimite-calcium sulfate system hydration [32,34–36]. First of all, Fig. 7b displays the calculated hydration degree, α given by equation (E.1), of CSA-sol and CSA-chem pastes. After 3 days, CSA-chem paste reaches more than 96.3 % while it is almost 72.4 % for the CSA-sol paste. After 7 days, the degree of reaction reached 97.6 % and 79.9 % for CSA-chem and CSA-sol, respectively. Finally, it was observed that at 28 days, the hydration of Ye-chem was nearly complete reaching almost 98 % hydration degree, while Ye-sol hydration degree attains only 88.7 %. Concerning the hydrates, the quantities are higher at any time in CSA-chem than in CSA-sol.

TGA curves are presented in Fig. 7c. Weight loss between 80 and 150°C can be assigned to ettringite decomposition (Zone II, Fig. 7c) [27,36]. Gypsum can decompose between 150 and 220°C (Zone III, Fig. 7c) [27,36]. Weight loss between 100 and 800°C can originate from the decomposition of monosulfoaluminate (Zones II, III, and IV, Fig. 7c), with a maximum decomposition at 200°C [27,34]. Lastly, between 200 and 300°C, the weight loss associated to the decomposition of gibbsite can be detected (Zone IV, Fig. 7c) [27,36]. Despite an overlap between the decomposition of the different products with temperature, TGA results (Fig. 7c) show higher total weight loss for CSA-chem compared to CSA-sol, at all hydration durations, which comes mainly from the decomposition of hydrates. In conclusion, TGA and XRD results give similar trends: the finer the ye'elimite powder, the faster the cement containing this powder hydrates. The presence of nano-grains of ye'elimite stimulates nucleation processes during the early cement hydration. The earlier these nuclei are formed, the earlier they can grow to larger crystals of hydrated phases and thereby accelerates the cement hydration [17]. Moreover, the high dissolution rate of nano-grains of ye'elimite probably leads to higher saturation index with respect to the different hydrates during the first days of hydration [28].

3.4. Influence of citric acid on CSA model cements hydration

The evolution of phases of the CSA-sol pastes, in the presence of different citric acid dosages (0 wt.%, 0.5 wt.% and 1 wt.%) and for different curing ages (3 days, 7 days and 28 days), were

followed by XRD (Fig. 8a) with the corresponding Rietveld results (Table 6). Again, we will focus for clarity on the amount of remaining ye'elimite and on the total quantities of formed hydrates (ettringite, the most abundant hydrate, monosulfoaluminate and gibbsite). The nature of the formed hydrate phases is in accordance with experimental results previously published about CSA cement hydration in the presence citric acid [5,6]. The variations of the calculated hydration degree, α given by equation (E.1), of CSA-sol pastes containing different citric acid dosages are presented in Fig. 8b. The results show that citrate retards the hydration: CSA-sol-0 reacts at a faster pace after 3 days since the degree of hydration of ye'elimite is 72.4 %, while CSA-sol-0.5 and CSA-sol-1 pastes reach only 66.6 % and 17.0 %, respectively. After 7 days, CSA-sol-0, CSA-sol-0.5 and CSA-sol-1 reach more than 79.9 %, almost 73.2 % and 26.4 % degree of hydration, respectively. Lastly, after 28 days of hydration, the figures are 88.7 %, almost 75.6 % and 65.2 % for CSA-sol-0, CSA-sol-0.5 and CSA-sol-1 respectively. Therefore, the major effect of citric acid addition on ye'elimite hydration is the slowing down of the hydration kinetics of the cement paste, suggesting an adsorption of citrate molecules on ye'elimite grains. In (section 3-2), it was explained how citric acid can delay ye'elimite dissolution by the possible citrate adsorption on ye'elimite grains. An analysis of TGA results (Fig. 8c) shows the same trend, i.e. a marked decrease of weight loss with the addition of citric acid, especially with 1 wt.%. The delay induced by citric acid on the reactivity of CSA-sol-0.5 and CSA-sol-1 can be explained by the fact that citrate molecules will bond with calcium on the surface of ye'elimite to give a chelate and interfere with ye'elimite dissolution, in addition to forming chelates with calcium ions already in solution, thus lowering their availability for participating in hydration reactions as it was already shown for OPC cement [9]. Citric acid addition lowers ettringite quantities (Table 6). In fact, some amounts of calcium and aluminium ions produced from ye'elimite and gypsum dissolution could form chelates with citrate, leading to the decease of the saturation index with respect to ettringite [28]. The absence of interaction between citrate and ettringite was proven in literature and it can be confirmed in the present case [8].

4. Conclusion

In order to contribute to the understanding of CSA concrete characteristics, this work has examined the effect of fineness on hydration of ye'elimite powder, which is one component of CSA cements. Ye'elimite of two different finesses was prepared either by a solid state method or by a chemical route. The role of fineness on the hydration of two model CSA cements and the effect of citric acid addition on the hydration of a CSA model cement were examined. The main conclusions of the present work can be summarized as follows.

The main difference found between the dissolution of ye'elimite powders prepared by chemical or solid state routes is related to the reaction rate. The presence of fine grains (100 to 200 nm) of ye'elimite accelerates the dissolution. From an industrial point of view, the presence of a fine fraction of ye'elimite grains (of the order of 100 – 200 nm) formed after grinding a commercial CSA clinker can considerably accelerate the hydration and therefore the expansion behavior. The presence of nano-grains of ye'elimite stimulates nucleation processes during the early cement hydration. The earlier these nuclei are formed, the earlier they can develop into large crystals of hydrated phases and thereby accelerate the cement hydration. Moreover, the high dissolution rate of nano-grains of ye'elimite probably leads to higher saturation index with respect to the different hydrates during the first days of hydration.

The addition of citric acid to the mixing water leads to a retarding effect on the dissolution of ye'elimite grains. Also, the surface of the grains presents scarce etch pits when citric acid is present in the water, while the surface seems to be totally attacked with water. These results indicate that the hydration of CSA model cements prepared from the mixing of ye'elimite powder – prepared by solid state reaction - and gypsum is retarded in the presence of citric acid at concentrations of 0.5 wt.% and 1 wt.% with respect to ye'elimite. Citric acid may work efficiently as a retarding additive for CSA cements since it slows down the initial ye'elimite dissolution. In the present work, it was also shown that the addition of citric acid with CSA model cements delays the formation of hydrates, especially ettringite. The delay effect of citric acid can be explained by the fact that citrate molecules

form chelates with calcium on the surface of ye'elimite and interfere with ye'elimite dissolution, in addition to forming chelates with calcium ions already in solution, thus lowering their availability for participating in hydration reactions.

Expansion behavior of commercial CSA cements could be controlled by the addition of citric acid, because it is well known that the fresh CSA concrete properties depend mainly on ettringite quantities in the hydrated cement pastes.

In conclusion, powder fineness and citric acid addition are two levers that could be helpful for industrial CSA cement producers, because they constitute a practical way to control the amount of formed ettringite, and hence the expansion behaviour of CSA cements. The influence of ye'elimite powder fineness and citric acid addition on the dimensional stability, workability, mechanical properties and durability performances of CSA cements and concretes could be the subject of further studies.

References

[1] F.P. Glasser, L. Zhang, High-performance cement matrices based on calcium sulfoaluminate–belite compositions, Cem. Concr. Res. 31 (2001) 1881–1886.

[2] R. Trauchessec, J.-M. Mechling, A. Lecomte, A. Roux, B. Le Rolland, Hydration of ordinary Portland cement and calcium sulfoaluminate cement blends, Cem. Concr. Compos. 56 (2015) 106–114.

[3] M.C.G. Juenger, F. Winnefeld, J.L. Provis, J.H. Ideker, Advances in alternative cementitious binders, Cem. Concr. Res. 41 (2011) 1232–1243.

[4] L.E. Burris, K.E. Kurtis, Influence of set retarding admixtures on calcium sulfoaluminate cement hydration and property development, Cem. Concr. Res. 104 (2018) 105–113.

[5] J. Tinnea, J.F. Young, Influence of Citric Acid on Reactions in the System 3CaO·Al2O3-CaSO4·2H2O-CaO-H2O, J. Am. Ceram. Soc. 60 (1977) 387–389. https://doi.org/10.1111/j.1151-2916.1977.tb15518.x.

[6] F. Winnefeld, S. Klemm, Influence of citric acid on the hydration kinetics of calcium sulfoaluminate cement, in: Submitt. First Int. Conf. Sulphoaluminate Cem. Mater. Eng. Technol. Wuhan China, 2013.

[7] M. Zajac, J. Skocek, F. Bullerjahn, M. Ben Haha, Effect of retarders on the early hydration of calcium-sulpho-aluminate (CSA) type cements, Cem. Concr. Res. 84 (2016) 62–75. https://doi.org/10.1016/j.cemconres.2016.02.014.

[8] A.M. Cody, H. Lee, R.D. Cody, P.G. Spry, The effects of chemical environment on the nucleation, growth, and stability of ettringite [Ca3Al (OH) 6] 2 (SO4) 3· 26H2O, Cem. Concr. Res. 34 (2004) 869–881.

[9] M. Prisciandaro, A. Lancia, D. Musmarra, The retarding effect of citric acid on calcium sulfate nucleation kinetics, Ind. Eng. Chem. Res. 42 (2003) 6647–6652.

[10] J.-B. Champenois, M. Dhoury, C.C.D. Coumes, C. Mercier, B. Revel, P. Le Bescop, D. Damidot, Influence of sodium borate on the early age hydration of calcium sulfoaluminate cement, Cem. Concr. Res. 70 (2015) 83–93.
[11] G. Zhang, G. Li, Y. Li, Effects of superplasticizers and retarders on the fluidity and strength of sulphoaluminate cement, Constr. Build. Mater. 126 (2016) 44–54.
[12] F. Sajedi, H.A. Razak, Effects of curing regimes and cement fineness on the compressive strength of ordinary Portland cement mortars, Constr. Build. Mater. 25 (2011) 2036–2045.
[13] E.H. Kadri, S. Aggoun, G. De Schutter, K. Ezziane, Combined effect of chemical nature and fineness of mineral powders on Portland cement hydration, Mater. Struct. 43 (2010) 665–673.
[14] E.C. Higginson, The effect of cement fineness on concrete, in: Fineness Cem., ASTM International, 1970.
[15] K.M. Alexander, The relationship between strength and the composition and fineness of cement, Cem. Concr. Res. 2 (1972) 663–680.
[16] J. Hu, Z. Ge, K. Wang, Influence of cement fineness and water-to-cement ratio on mortar early-age heat of hydration and set times, Constr. Build. Mater. 50 (2014) 657–663.
[17] G. Land, D. Stephan, Controlling cement hydration with nanoparticles, Cem. Concr. Compos. 57 (2015) 64–67.
[18] J.-T. Song, J.F. Young, Direct synthesis and hydration of calcium aluminosulfate (Ca4Al6O16S), J. Am. Ceram. Soc. 85 (2002) 535–539.
[19] J.J. Thomas, S. Ghazizadeh, E. Masoero, Kinetic mechanisms and activation energies for hydration of standard and highly reactive forms of β-dicalcium silicate (C2S), Cem. Concr. Res. 100 (2017) 322–328.
[20] H. Pöllmann, Cementitious Materials: Composition, Properties, Application, Walter de Gruyter GmbH & Co KG, 2017.
[21] S.-H. Hong, J.F. Young, Hydration kinetics and phase stability of dicalcium silicate synthesized by the Pechini process, J. Am. Ceram. Soc. 82 (1999) 1681–1686.
[22] D.A. Fumo, M.R. Morelli, A.M. Segadaes, Combustion synthesis of calcium aluminates, Mater. Res. Bull. 31 (1996) 1243–1255.
[23] P.K. Mehta, Mechanism of expansion associated with ettringite formation, Cem. Concr. Res. 3 (1973) 1–6.
[24] K. Ogawa, D.M. Roy, C4A3S hydration ettringite formation, and its expansion mechanism: I. expansion; Ettringite stability, Cem. Concr. Res. 11 (1981) 741–750.
[25] Y. El Khessaimi, Y. El Hafiane, A. Smith, R. Trauchessec, C. Diliberto, A. Lecomte, Solid-state synthesis of pure ye'elimite, J. Eur. Ceram. Soc. 38 (2018) 3401–3411.
[26] H. Le Chatelier, Recherches expérimentales sur la constitution des mortiers hydrauliques, Dunod, 1904.
[27] F. Winnefeld, S. Barlag, Calorimetric and thermogravimetric study on the influence of calcium sulfate on the hydration of ye'elimite, J. Therm. Anal. Calorim. 101 (2009) 949–957.
[28] F. Winnefeld, B. Lothenbach, Hydration of calcium sulfoaluminate cements—experimental findings and thermodynamic modelling, Cem. Concr. Res. 40 (2010) 1239–1247.
[29] R. Trauchessec, J.-M. Mechling, A. Lecomte, A. Roux, B. Le Rolland, Impact of anhydrite proportion in a calcium sulfoaluminate cement and Portland cement blend, Adv. Cem. Res. 26 (2014) 325–333.
[30] F. Hanic, I. Kaprálik, A. Gabrisová, Mechanism of hydration reactions in the system C4A3S□ CS□ CaO□ H2O referred to hydration of sulphoaluminate cements, Cem. Concr. Res. 19 (1989) 671–682.
[31] C.W. Hargis, A.P. Kirchheim, P.J. Monteiro, E.M. Gartner, Early age hydration of calcium sulfoaluminate (synthetic ye'elimite, C4A3S) in the presence of gypsum and varying amounts of calcium hydroxide, Cem. Concr. Res. 48 (2013) 105–115.

[32] F. Bullerjahn, E. Boehm-Courjault, M. Zajac, M. Ben Haha, K. Scrivener, Hydration reactions and stages of clinker composed mainly of stoichiometric ye'elimite, Cem. Concr. Res. 116 (2019) 120–133. https://doi.org/10.1016/j.cemconres.2018.10.023.
[33] M. Zajac, J. Skocek, F. Bullerjahn, B. Lothenbach, K. Scrivener, M.B. Haha, Early hydration of ye'elimite: Insights from thermodynamic modelling, Cem. Concr. Res. 120 (2019) 152–163.
[34] A. Cuesta, G. Álvarez-Pinazo, S.G. Sanfélix, I. Peral, M.A. Aranda, A.G. De la Torre, Hydration mechanisms of two polymorphs of synthetic ye'elimite, Cem. Concr. Res. 63 (2014) 127–136.
[35] D. Jansen, A. Spies, J. Neubauer, D. Ectors, F. Goetz-Neunhoeffer, Studies on the early hydration of two modifications of ye'elimite with gypsum, Cem. Concr. Res. 91 (2017) 106–116.
[36] F. Bullerjahn, M. Zajac, M.B. Haha, K.L. Scrivener, Factors influencing the hydration kinetics of ye'elimite; effect of mayenite, Cem. Concr. Res. 116 (2019) 113–119.
[37] C.W. Hargis, A. Telesca, P.J.M. Monteiro, Calcium sulfoaluminate (Ye'elimite) hydration in the presence of gypsum, calcite, and vaterite, Cem. Concr. Res. 65 (2014) 15–20. https://doi.org/10.1016/j.cemconres.2014.07.004.
[38] M.B. Haha, F. Winnefeld, A. Pisch, Advances in understanding ye'elimite-rich cements, Cem. Concr. Res. 123 (2019) 105778.
[39] Y. El Khessaimi, Y. El Hafiane, A. Smith, Ye'elimite synthesis by chemical routes, J. Eur. Ceram. Soc. 39 (2019) 1683–1695.
[40] X. Li, Y. Zhang, X. Shen, Q. Wang, Z. Pan, Kinetics of calcium sulfoaluminate formation from tricalcium aluminate, calcium sulfate and calcium oxide, Cem. Concr. Res. 55 (2014) 79–87.
[41] A. Cuesta, A.G. De la Torre, I. Santacruz, P. Trtik, J.C. Da Silva, A. Diaz, M. Holler, M.A. Aranda, Chemistry and mass density of aluminum hydroxide gel in eco-cements by ptychographic x-ray computed tomography, J. Phys. Chem. C. 121 (2017) 3044–3054.
[42] Y. El Khessaimi, Y. El Hafiane, A. Smith, Examination of ye'elimite formation mechanisms, J. Eur. Ceram. Soc. 39 (2019) 5086–5095.
[43] Á.G. De la Torre, I. Santacruz, L. León-Reina, A. Cuesta, M.A.G. Aranda, 1. Diffraction and crystallography applied to anhydrous cements, in: H. Pöllmann (Ed.), Cem. Mater., De Gruyter, Berlin, Boston, 2017: pp. 3–30. doi:10.1515/9783110473728-002., in: n.d.
[44] A. Cuesta, A.G. De la Torre, E.R. Losilla, V.K. Peterson, P. Rejmak, A. Ayuela, C. Frontera, M.A. Aranda, Structure, atomistic simulations, and phase transition of stoichiometric yeelimite, Chem. Mater. 25 (2013) 1680–1687.
[45] F. Goetz-Neunhoeffer, J. Neubauer, Refined ettringite (Ca 6 Al 2 (SO 4) 3 (OH) 12· 26H 2 O) structure for quantitative X-ray diffraction analysis, Powder Diffr. 21 (2006) 4–11.
[46] R. Allmann, Refinement of the hybrid layer structure [Ca2Al (OH) 6]+·[1/2SO4· 3H2O]-, Neues Jahrb. Für Mineral. Monatshefte. 1977 (1977) 136–143.
[47] H. Saalfeld, M. Wedde, Refinement of the crystal structure of gibbsite, A1 (OH) 3, Z. Für Krist.-Cryst. Mater. 139 (1974) 129–135.
[48] G. Angeles, M.-G. López-Olmo, C. Alvarez-Rua, S. García-Granda, M.A. Aranda, Structure and microstructure of gypsum and its relevance to Rietveld quantitative phase analyses, Powder Diffr. 19 (2004) 240–246.
[49] B.H. Toby, R factors in Rietveld analysis: how good is good enough?, Powder Diffr. 21 (2006) 67–70.
[50] A. Cuesta, A.G. De la Torre, I. Santacruz, P. Trtik, J.C. Da Silva, A. Diaz, M. Holler, M.A. Aranda, Chemistry and mass density of aluminum hydroxide gel in eco-cements by ptychographic x-ray computed tomography, J. Phys. Chem. C. 121 (2017) 3044–3054.
[51] G. Álvarez-Pinazo, A. Cuesta, M. García-Maté, I. Santacruz, E.R. Losilla, A.G. De la Torre, L. León-Reina, M.A. Aranda, Rietveld quantitative phase analysis of Yeelimite-containing cements, Cem. Concr. Res. 42 (2012) 960–971.
[52] R. Trauchessec, Mélanges de ciments sulfoalumineux et Portland, PhD Thesis, Université de Lorraine, 2013.

612 [53] L. Pelletier, F. Winnefeld, B. Lothenbach, The ternary system Portland cement–calcium
613 sulphoaluminate clinker–anhydrite: hydration mechanism and mortar properties, Cem. Concr.
614 Compos. 32 (2010) 497–507.
615 [54] W. Hanley, D. Constantiner, J. Goldbrunner, Retarder for calcium sulfoaluminate cements,
616 2004.
617 [55] T. EN, 196-1. Methods of testing cement–Part 1: Determination of strength, Eur. Comm.
618 Stand. 26 (2005).
619 [56] P. Juilland, E. Gallucci, R. Flatt, K. Scrivener, Dissolution theory applied to the induction period
620 in alite hydration, Cem. Concr. Res. 40 (2010) 831–844.
621 https://doi.org/10.1016/j.cemconres.2010.01.012.
622 [57] P. Juilland, E. Gallucci, Morpho-topological investigation of the mechanisms and kinetic
623 regimes of alite dissolution, Cem. Concr. Res. 76 (2015) 180–191.
624 https://doi.org/10.1016/j.cemconres.2015.06.001.
625 [58] L. Nicoleau, A. Nonat, D. Perrey, The di- and tricalcium silicate dissolutions, Cem. Concr. Res.
626 47 (2013) 14–30. https://doi.org/10.1016/j.cemconres.2013.01.017.
627 [59] P. Barret, D. Ménétrier, Filter dissolution of C3S as a function of the lime concentration in a
628 limited amount of lime water, Cem. Concr. Res. 10 (1980) 521–534.
629 [60] A.C. Lasaga, A. Luttge, Variation of crystal dissolution rate based on a dissolution stepwave
630 model, Science. 291 (2001) 2400–2404.
631 [61] P.M. Dove, N. Han, Kinetics of mineral dissolution and growth as reciprocal microscopic
632 surface processes across chemical driving force, in: AIP Conf. Proc., AIP, 2007: pp. 215–234.
633 [62] P.M. Dove, N. Han, J.J. De Yoreo, Mechanisms of classical crystal growth theory explain quartz
634 and silicate dissolution behavior, Proc. Natl. Acad. Sci. 102 (2005) 15357–15362.
635 [63] A.C. Lasaga, Kinetic theory in the earth sciences, Princeton university press, 2014.
636 [64] T.E. Burch, K.L. Nagy, A.C. Lasaga, Free energy dependence of albite dissolution kinetics at
637 80°C and pH 8.8, Chem. Geol. 105 (1993) 137–162. https://doi.org/10.1016/0009-
638 2541(93)90123-Z.
639 [65] R.N. Goldberg, N. Kishore, R.M. Lennen, Thermodynamic quantities for the ionization
640 reactions of buffers, J. Phys. Chem. Ref. Data. 31 (2002) 231–370.
641 [66] D.B. Emmert, P.J. Stoehr, G. Stoesser, G.N. Cameron, The European bioinformatics institute
642 (EBI) databases, Nucleic Acids Res. 22 (1994) 3445–3449.
643 [67] A. Cuesta, A.G. De la Torre, E.R. Losilla, V.K. Peterson, P. Rejmak, A. Ayuela, C. Frontera,
644 M.A.G. Aranda, Structure, Atomistic Simulations, and Phase Transition of Stoichiometric
645 Yeelimite, Chem. Mater. 25 (2013) 1680–1687. https://doi.org/10.1021/cm400129z.
646 [68] J.-P. Boisvert, M. Domenech, A. Foissy, J. Persello, J.-C. Mutin, Hydration of calcium sulfate
647 hemihydrate (CaSO4· 12H2O) into gypsum (CaSO4· 2H2O). The influence of the sodium poly
648 (acrylate)/surface interaction and molecular weight, J. Cryst. Growth. 220 (2000) 579–591.
649 [69] A. Ersen, A. Smith, T. Chotard, Effect of malic and citric acid on the crystallisation of gypsum
650 investigated by coupled acoustic emission and electrical conductivity techniques, J. Mater. Sci.
651 41 (2006) 7210–7217.
652 [70] E. Badens, S. Veesler, R. Boistelle, Crystallization of gypsum from hemihydrate in presence of
653 additives, J. Cryst. Growth. 198–199 (1999) 704–709. https://doi.org/10.1016/S0022-
654 0248(98)01206-8.
655 [71] J.P. Bombled, Rhéologie des mortiers et des bétons frais, influence du facteur ciment, in:
656 Proceeding RILEM Leeds Semin., 1973: pp. 1–169.
657 [72] A. Smith, Y. El Hafiane, J.-P. Bonnet, P. Quintard, B. Tanouti, Role of a small addition of acetic
658 acid on the setting behavior and on the microstructure of a calcium aluminate cement, J. Am.
659 Ceram. Soc. 88 (2005) 2079–2084.
660

Figure captions

Figure 1	(a) Calculated ye'elimite hydration degree (α%); Formed hydrates quantities relevant to Ettringite (b), Monosulfoaluminate (c) and Gibbsite (d); "w/c" refers to water by cement weight ratio; References: Cuesta et al.,2014 [34], Hargis et al.,2014 [37], Jansen et al.,2017 [35], Bullerjahn et al.,2019 [36], (α%) is given by equation (E.1).
Figure 2	Preparation protocol ye'elimite dissolution study of suspensions, (a) based on Ye-sol or Ye-chem, (b) based on Ye-sol with different citric acid percentages (0 wt.%, 5 wt.% and 10 wt.%).
Figure 3	Preparation protocol for hydration study of CSA model cement pastes, (a) based on Ye-sol or Ye-chem (blended with gypsum), or (b) based on Ye-sol (blended with gypsum) with different citric acid percentages (0 wt%, 0.5 wt.% and 1 wt.%).
Figure 4	(a) Ionic conductivity evolution of ye'elimite suspensions Ye-sol-0, Ye-chem, Ye-sol-5 and Ye-sol-10. All suspensions were prepared with w/c = 1000. t = 0 min in the graph's abscissa refers to the time when ye'elimite is added to the citric acid solution. (b) Ionic conductivity evolution of gypsum suspensions with different citric acid additions: 0 wt.% (Gy-0), 5 wt.% (Gy-5) and 10 wt.% (Gy-10). All suspensions were prepared with w/c = 1000. t = 0 min in the graph's abscissa refers to the time when gypsum is added to the citric acid solution.
Figure 5	SEM micrographs of Ye-sol-0 (a), Ye-sol-10 (b) and Ye-chem (c) suspensions. Observations were carried out after 1 min of hydration and all suspensions were prepared with W/C = 1000.
Figure 6	(a) Citric acid structure (CHEBI:30769) from the European Bioinformatics Institute Database [66], atoms are represented as spheres and are color coded as: carbon (grey), hydrogen (white) and oxygen (red). (b) Orthorhombic ye'elimite structure from Cuesta et al. [67] showing the $(13\bar{1})$ crystallographic plane, Ca denoted within dark-green spheres, Al within light blue

	tetrahedra, S within yellow tetrahedra, and O are red, for clarity CaO bonds are omitted in the represented structure.
Figure 7	XRD patterns (a), calculated hydration degree (α) (b), for CSA model cements (CSA-sol-0) and (CSA-Chem) at different hydration ages. E: ettringite; G: Gypsum; M: monosulfate; Y: ye'elimite; A: Gibssite, (α%) is given by equation (E.1), and TGA curves (c).
Figure 8	XRD patterns (a), calculated hydration degree (α) (b), for CSA model cements (CSA-sol-0), (CSA-sol-0.5) and (CSA-sol-1) at different hydration ages. E: ettringite; G: Gypsum; M: monosulfate; Y: ye'elimite; A: Gibssite. (α%) is given by equation (E.1), and TGA curves (c).

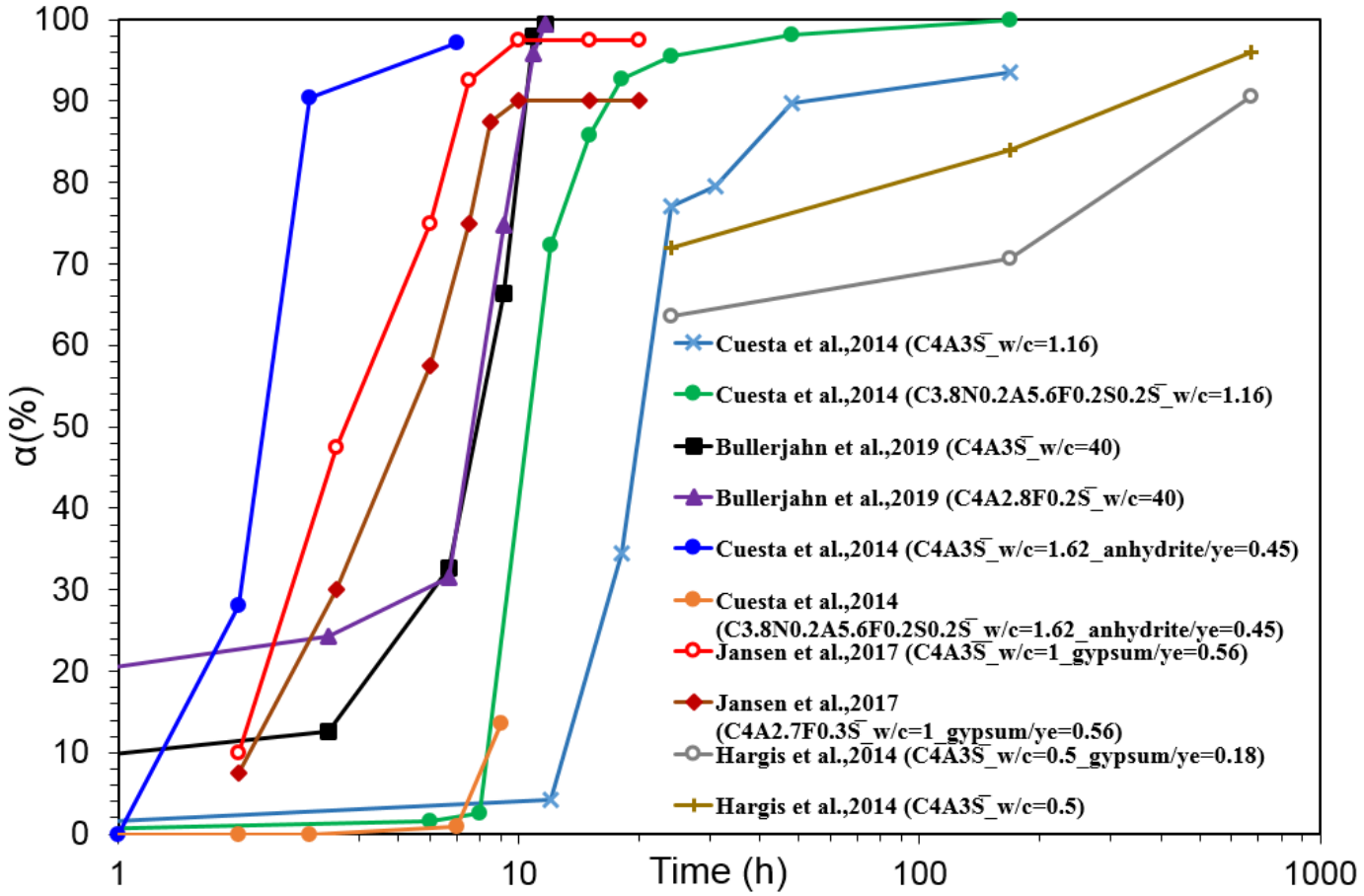

100
90
80
70
60
50
40
30
20
10
0
α(%)
1
10
Time (h)
100
1000
Cuesta et al.,2014 (C4A3S̄_w/c=1.16)
Cuesta et al.,2014 (C3.8N0.2A5.6F0.2S0.2S̄_w/c=1.16)
Bullerjahn et al.,2019 (C4A3S̄_w/c=40)
Bullerjahn et al.,2019 (C4A2.8F0.2S̄_w/c=40)
Cuesta et al.,2014 (C4A3S̄_w/c=1.62_anhydrite/ye=0.45)
Cuesta et al.,2014 (C3.8N0.2A5.6F0.2S0.2S̄_w/c=1.62_anhydrite/ye=0.45)
Jansen et al.,2017 (C4A3S̄_w/c=1_gypsum/ye=0.56)
Jansen et al.,2017 (C4A2.7F0.3S̄_w/c=1_gypsum/ye=0.56)
Hargis et al.,2014 (C4A3S̄_w/c=0.5_gypsum/ye=0.18)
Hargis et al.,2014 (C4A3S̄_w/c=0.5)

Figure 1-(a)

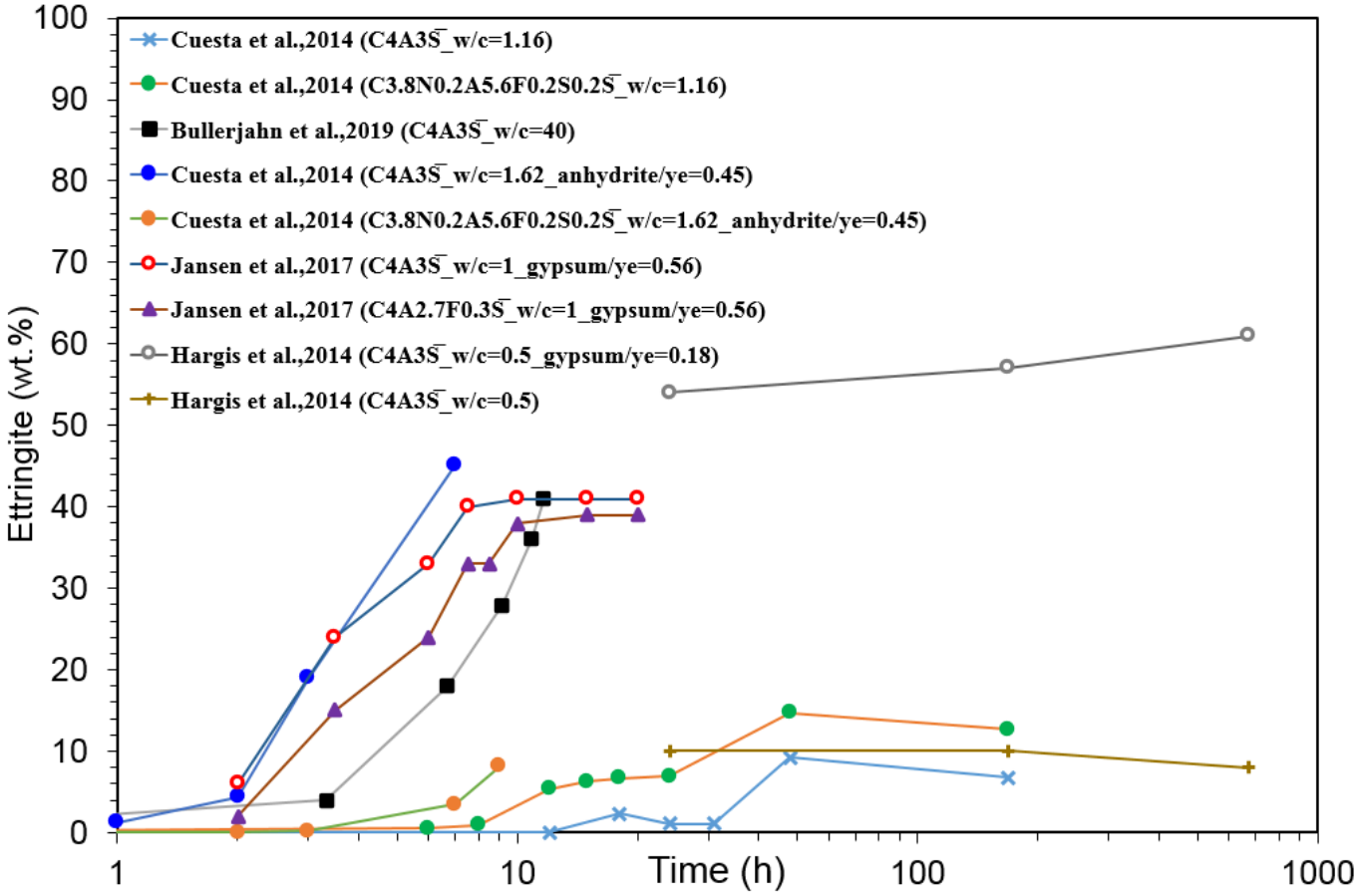

Cuesta et al.,2014 (C4A3S̄_w/c=1.16)
Cuesta et al.,2014 (C3.8N0.2A5.6F0.2S0.2S̄_w/c=1.16)
Bullerjahn et al.,2019 (C4A3S̄_w/c=40)
Cuesta et al.,2014 (C4A3S̄_w/c=1.62_anhydrite/ye=0.45)
Cuesta et al.,2014 (C3.8N0.2A5.6F0.2S0.2S̄_w/c=1.62_anhydrite/ye=0.45)
Jansen et al.,2017 (C4A3S̄_w/c=1_gypsum/ye=0.56)
Jansen et al.,2017 (C4A2.7F0.3S̄_w/c=1_gypsum/ye=0.56)
Hargis et al.,2014 (C4A3S̄_w/c=0.5_gypsum/ye=0.18)
Hargis et al.,2014 (C4A3S̄_w/c=0.5)
Ettringite (wt.%)
Time (h)
0
10
20
30
40
50
60
70
80
90
100
1
10
100
1000

Figure 1-(b)

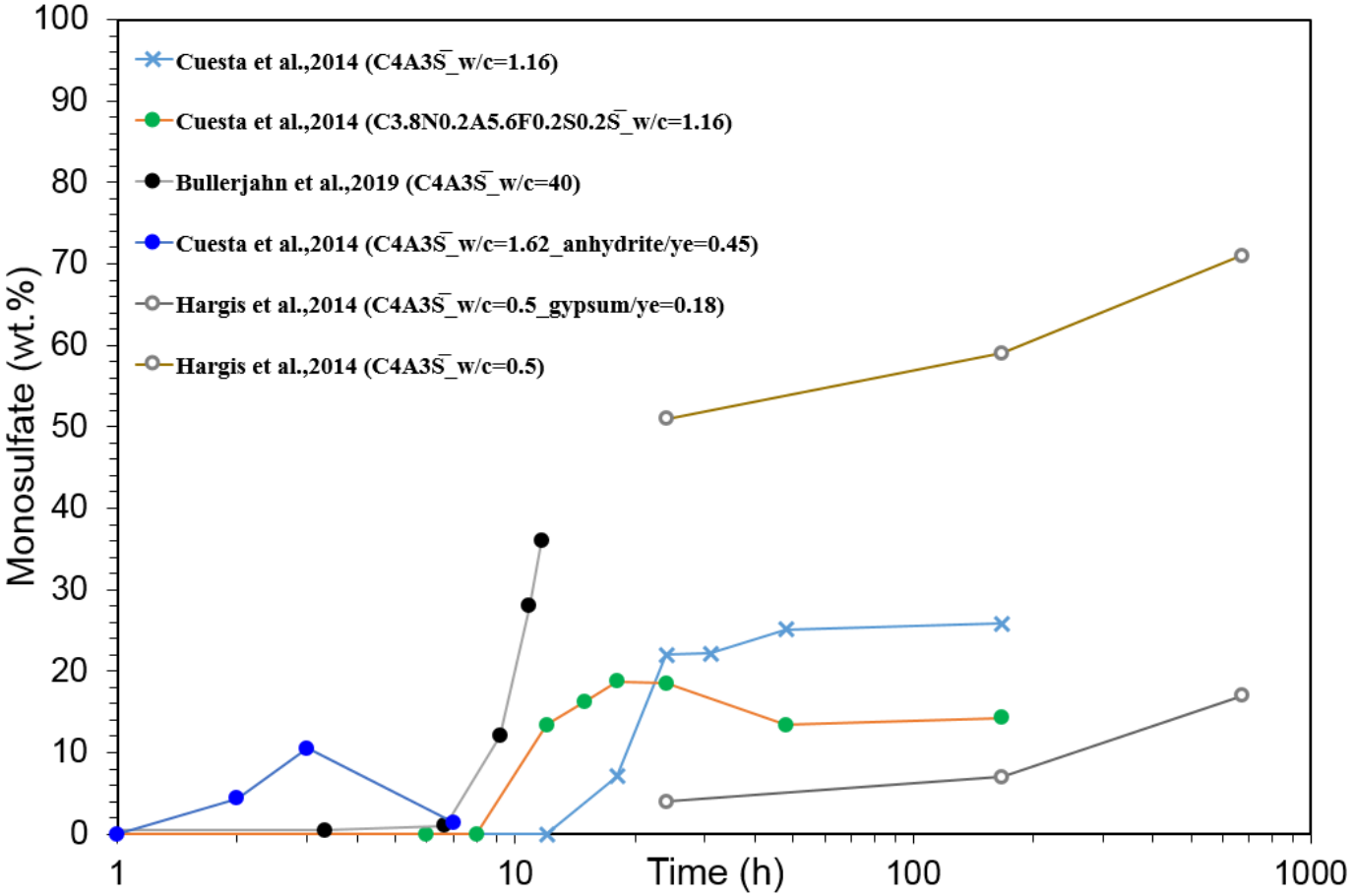

Cuesta et al.,2014 (C4A3S̄_w/c=1.16)
Cuesta et al.,2014 (C3.8N0.2A5.6F0.2S0.2S̄_w/c=1.16)
Bullerjahn et al.,2019 (C4A3S̄_w/c=40)
Cuesta et al.,2014 (C4A3S̄_w/c=1.62_anhydrite/ye=0.45)
Hargis et al.,2014 (C4A3S̄_w/c=0.5_gypsum/ye=0.18)
Hargis et al.,2014 (C4A3S̄_w/c=0.5)
Monosulfate (wt.%)
Time (h)
0
10
20
30
40
50
60
70
80
90
100
1
10
100
1000

Figure 1-(c)

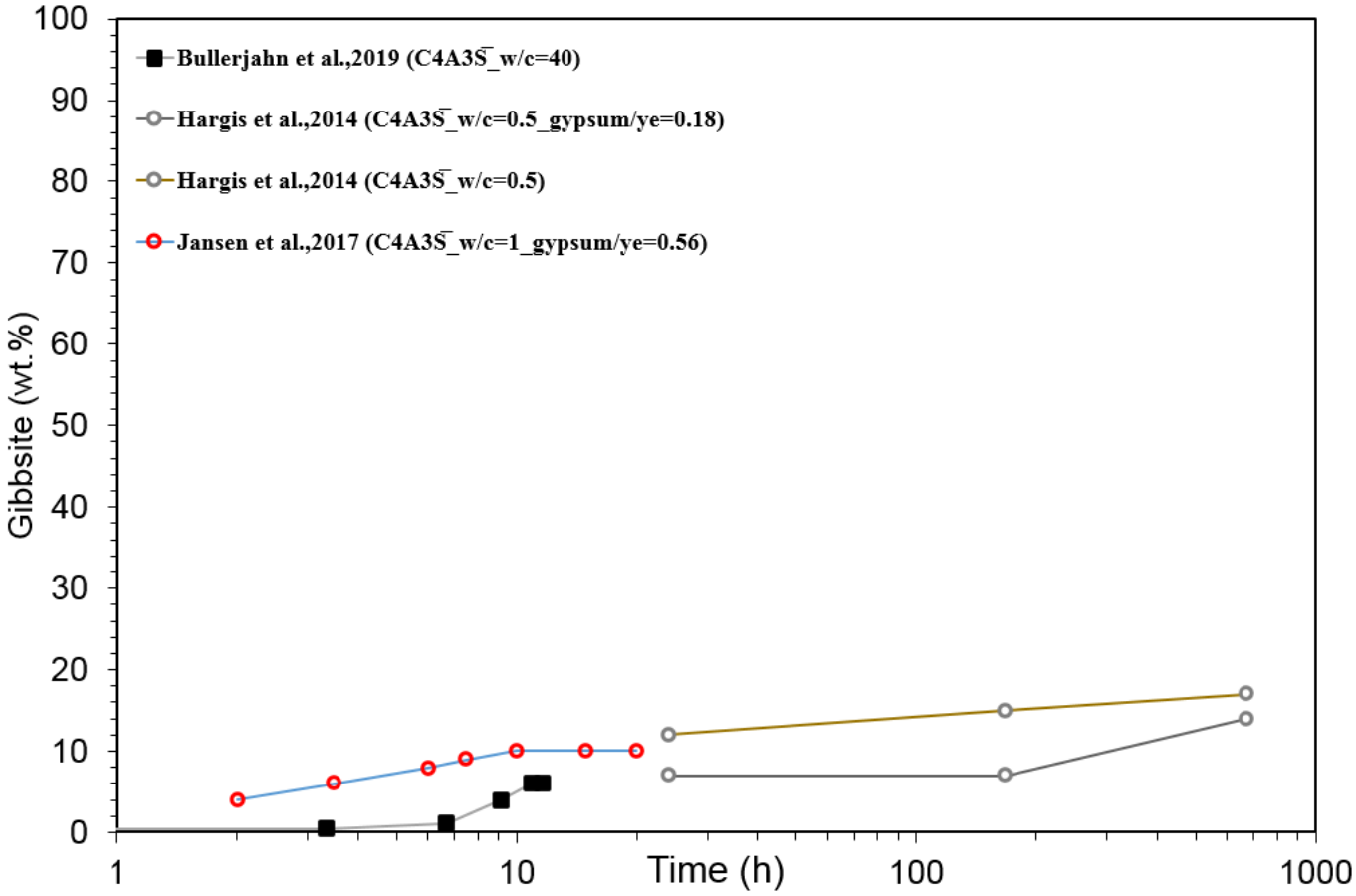

Bullerjahn et al.,2019 (C4A3S̄_w/c=40)
Hargis et al.,2014 (C4A3S̄_w/c=0.5_gypsum/ye=0.18)
Hargis et al.,2014 (C4A3S̄_w/c=0.5)
Jansen et al.,2017 (C4A3S̄_w/c=1_gypsum/ye=0.56)
Gibbsite (wt.%)
Time (h)
0
10
20
30
40
50
60
70
80
90
100
1
10
100
1000

Figure 1-(d)

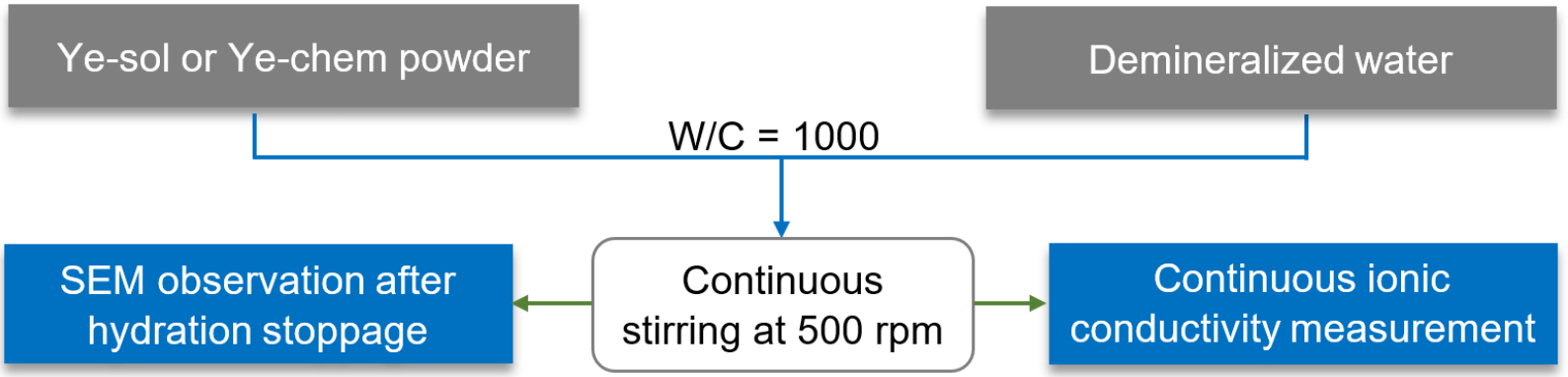


Figure 2a

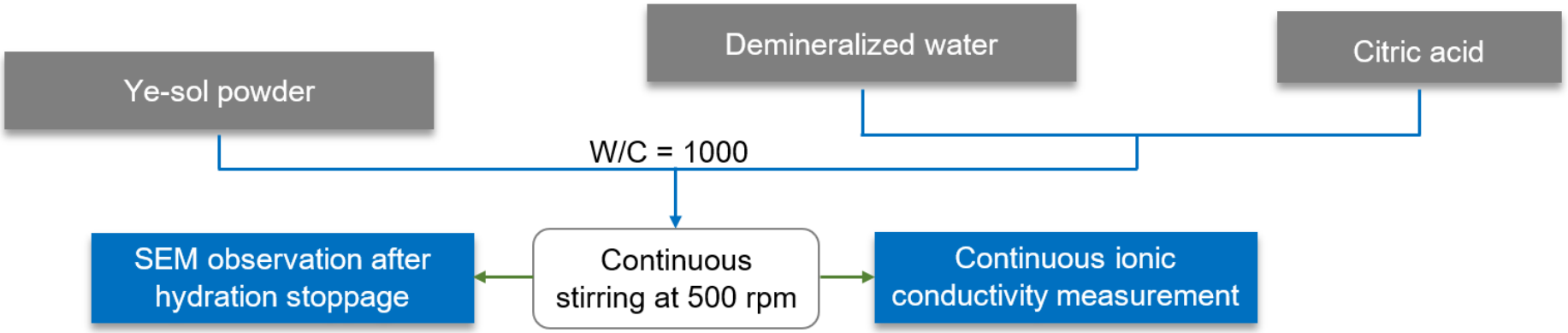


Figure 2b

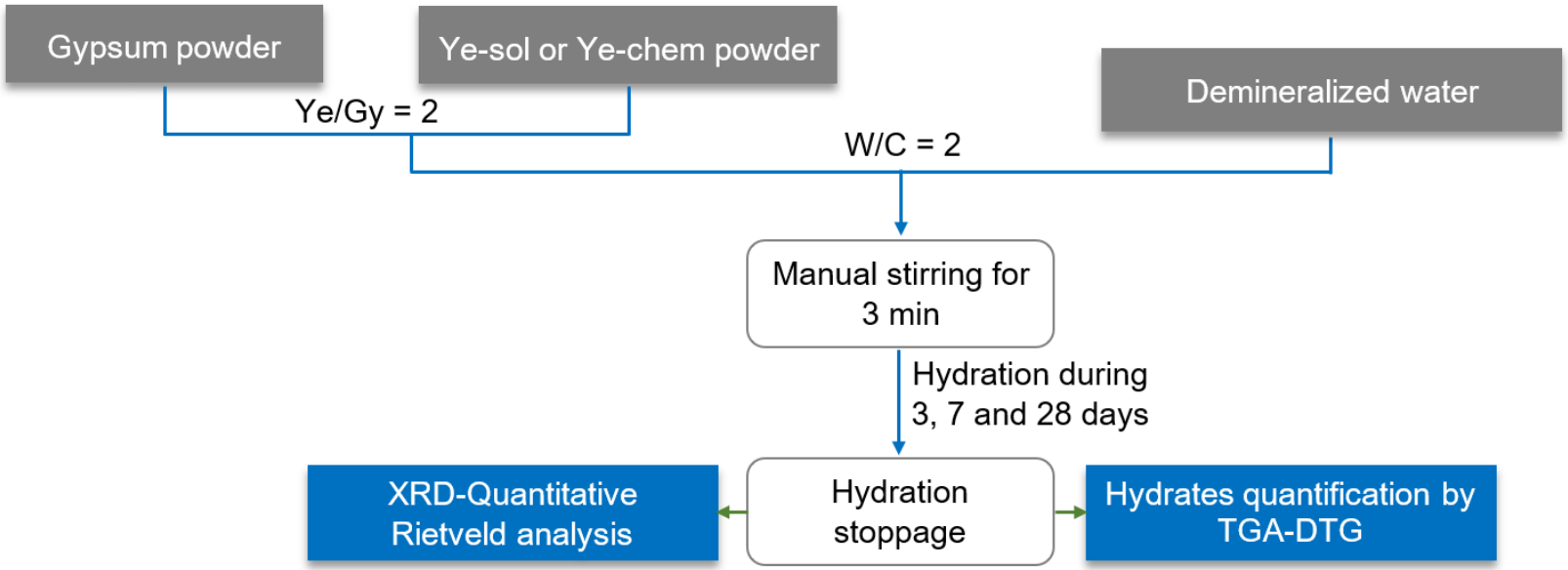

Gypsum powder
Ye-sol or Ye-chem powder
Ye/Gy = 2
Demineralized water
W/C = 2
Manual stirring for 3 min
Hydration during 3, 7 and 28 days
XRD-Quantitative Rietveld analysis
Hydration stoppage
Hydrates quantification by TGA-DTG

Figure 3a

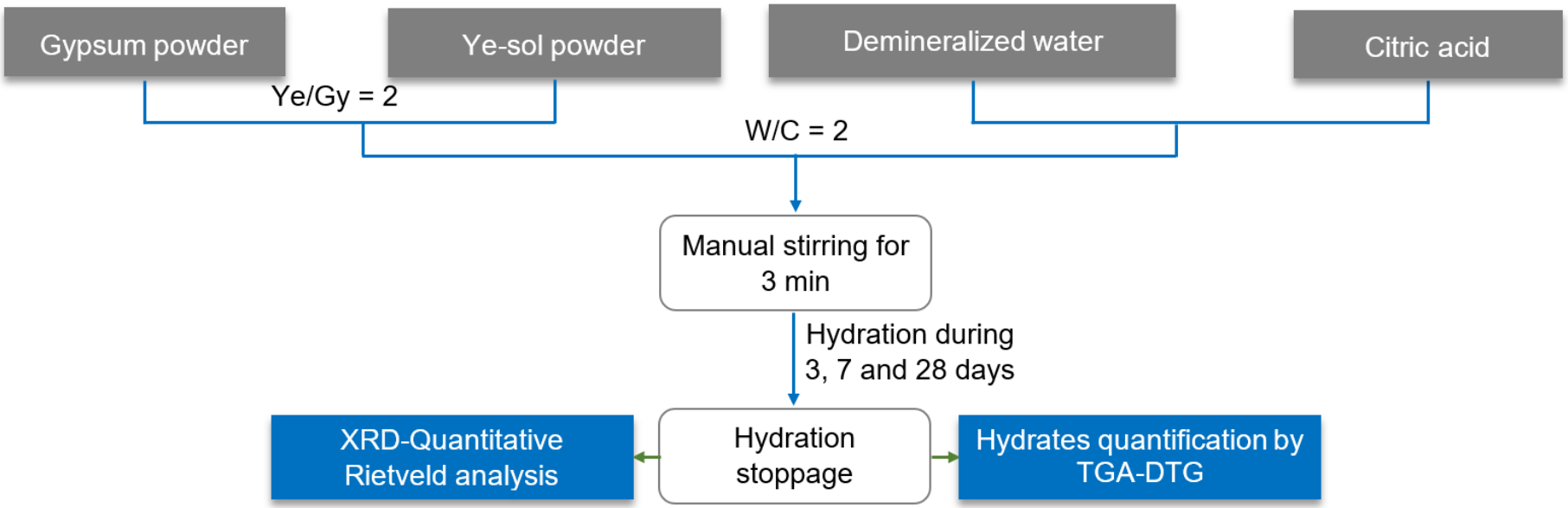

Gypsum powder
Ye-sol powder
Demineralized water
Citric acid
Ye/Gy = 2
W/C = 2
Manual stirring for 3 min
Hydration during 3, 7 and 28 days
XRD-Quantitative Rietveld analysis
Hydration stoppage
Hydrates quantification by TGA-DTG

Figure 3b

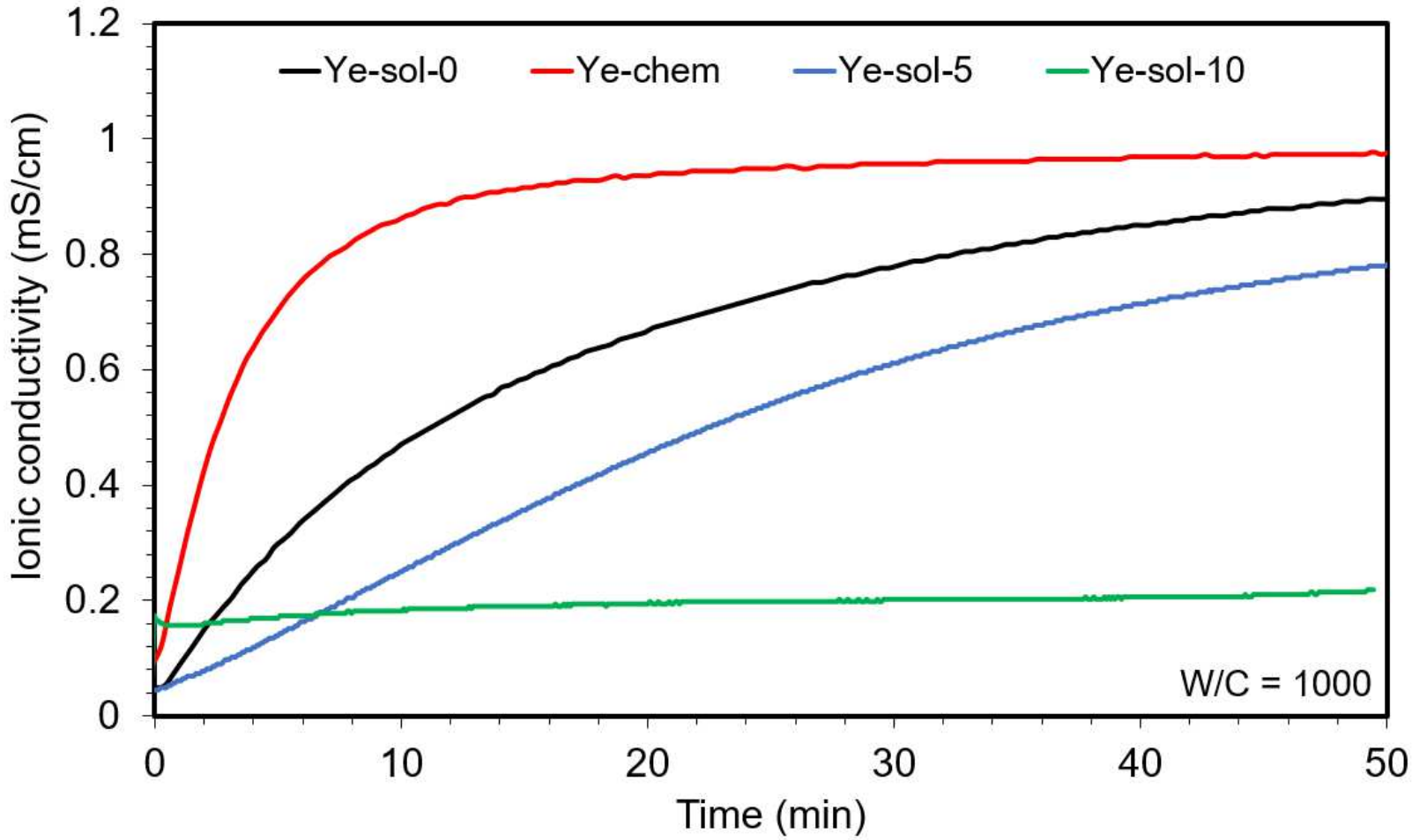

Ye-sol-0
Ye-chem
Ye-sol-5
Ye-sol-10
Ionic conductivity (mS/cm)
1.2
1
0.8
0.6
0.4
0.2
0
0
10
20
30
40
50
Time (min)
W/C = 1000

Figure 4a

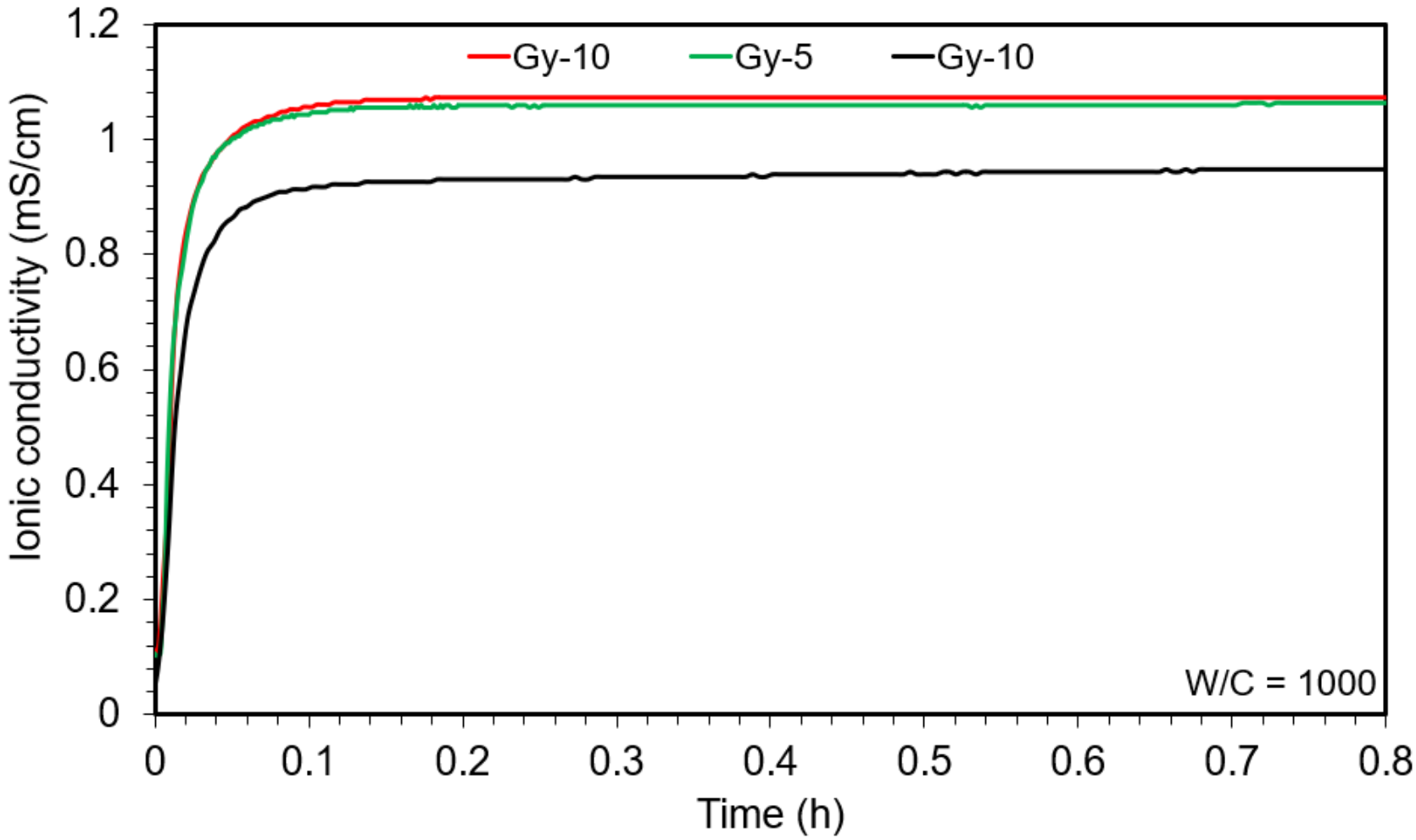
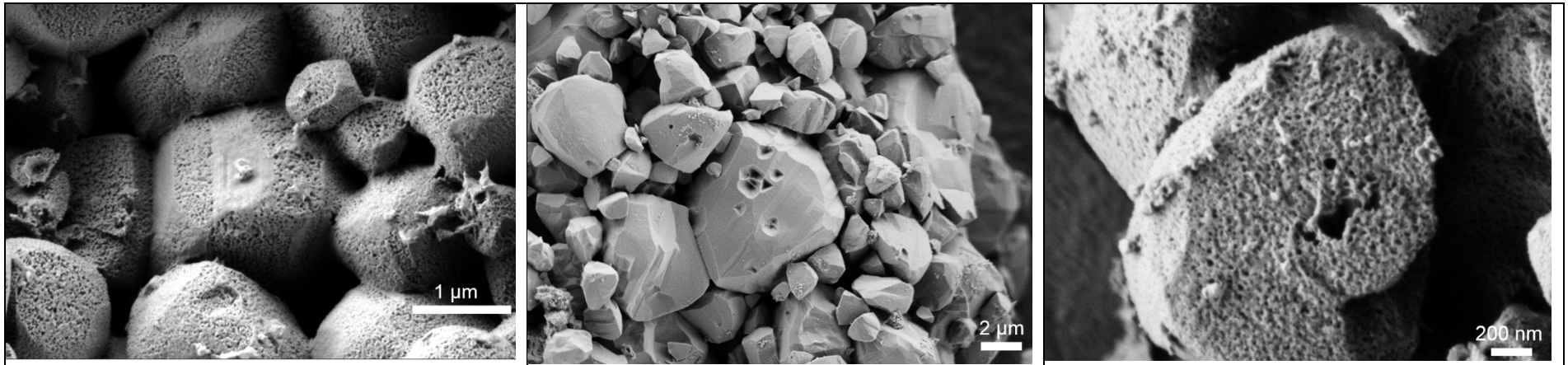

Gy-10
Gy-5
Gy-10
W/C = 1000
Ionic conductivity (mS/cm)
Time (h)
0
0.2
0.4
0.6
0.8
1
1.2
0
0.1
0.2
0.3
0.4
0.5
0.6
0.7
0.8

Figure 4b



(a) (b) (c)

Figure 5

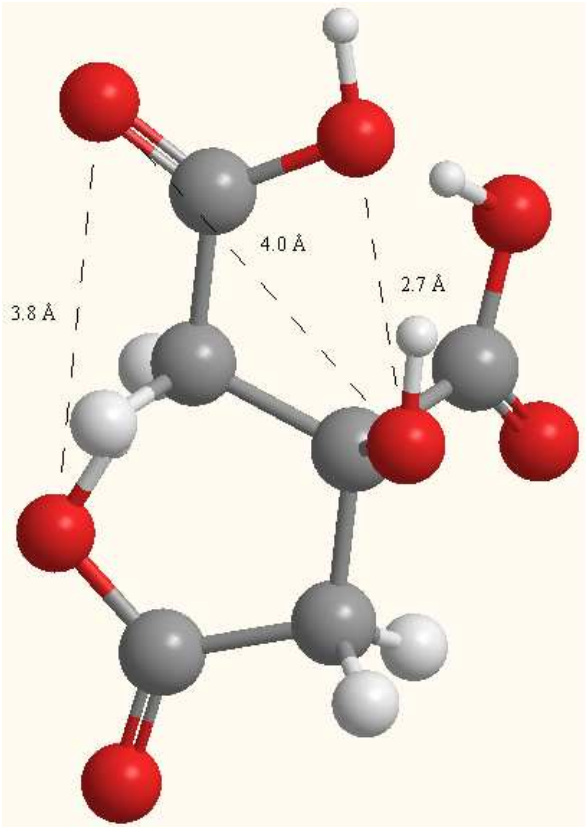


Figure 6 - (a)

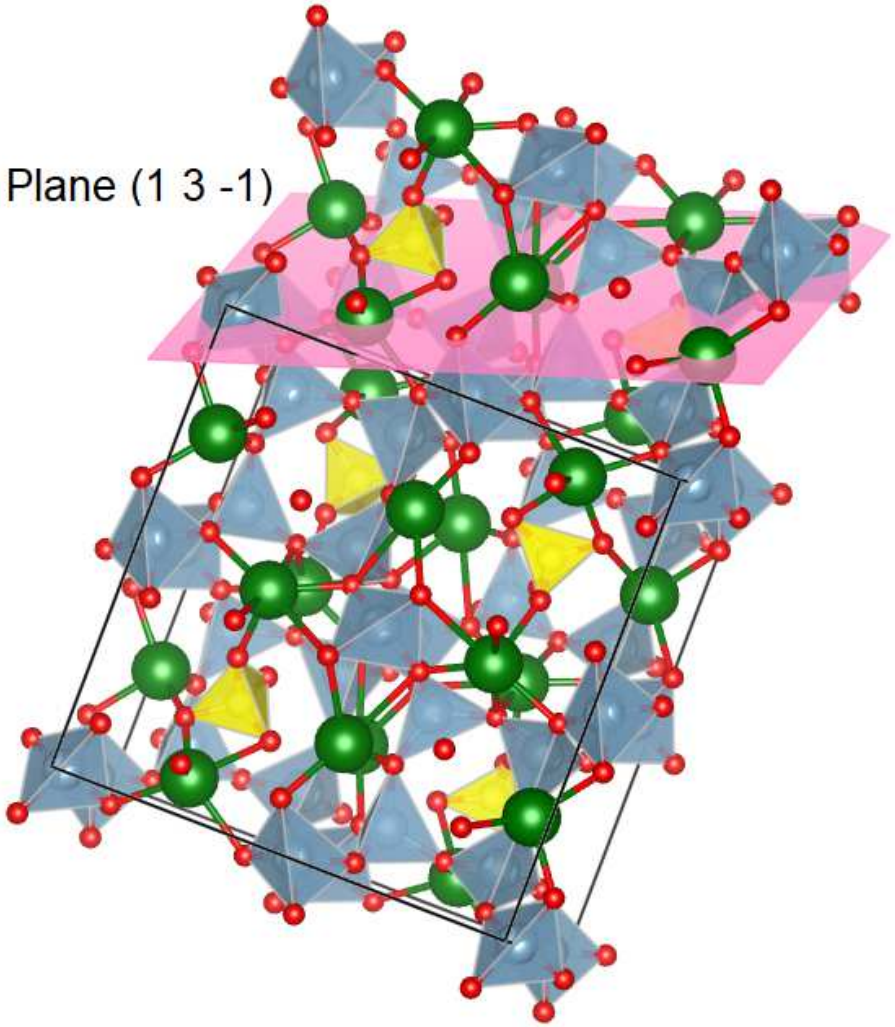


Figure 6 - (b)

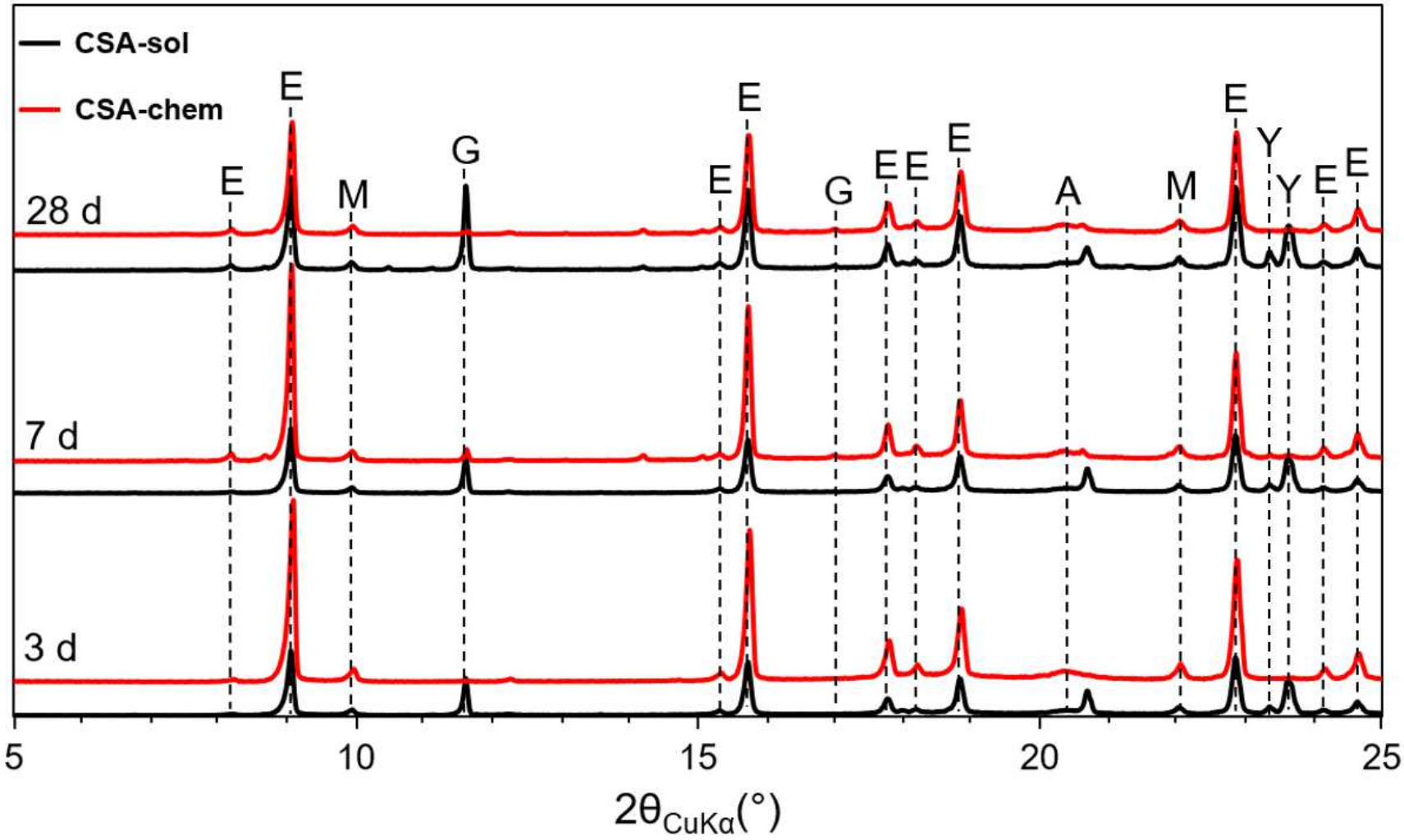

CSA-sol
CSA-chem
28 d
7 d
3 d
E
M
G
E
G
E
E
E
A
M
E
Y
Y
E
E
5
10
15
20
25
2θCuKα(°)

Figure 7 - (a)

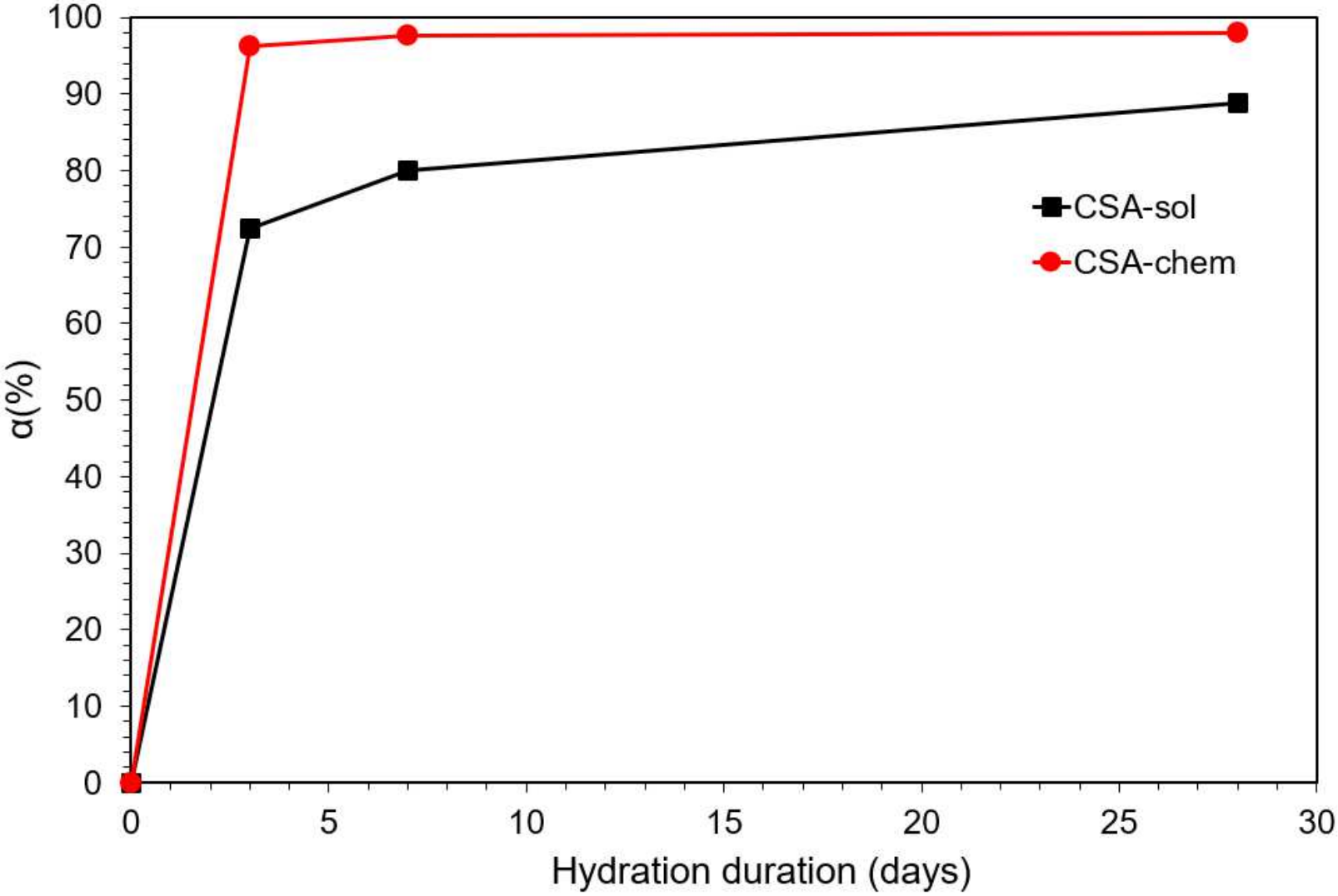

100
90
80
70
60
50
40
30
20
10
0
α(%)
0
5
10
15
20
25
30
Hydration duration (days)
CSA-sol
CSA-chem

Figure 7 - (b)

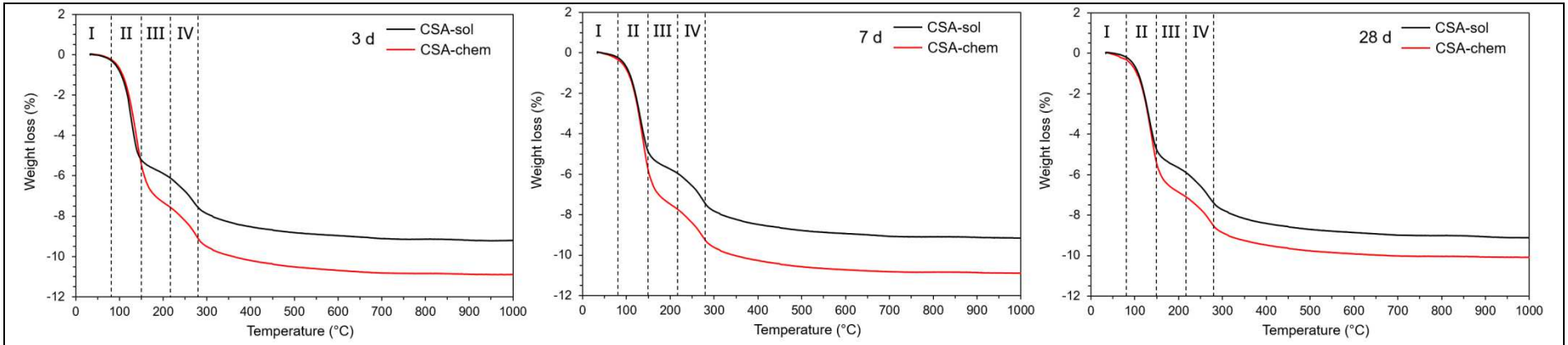

I
II
III
IV
3 d
7 d
28 d
CSA-sol
CSA-chem
Weight loss (%)
Temperature (°C)

Figure 7 - (c)

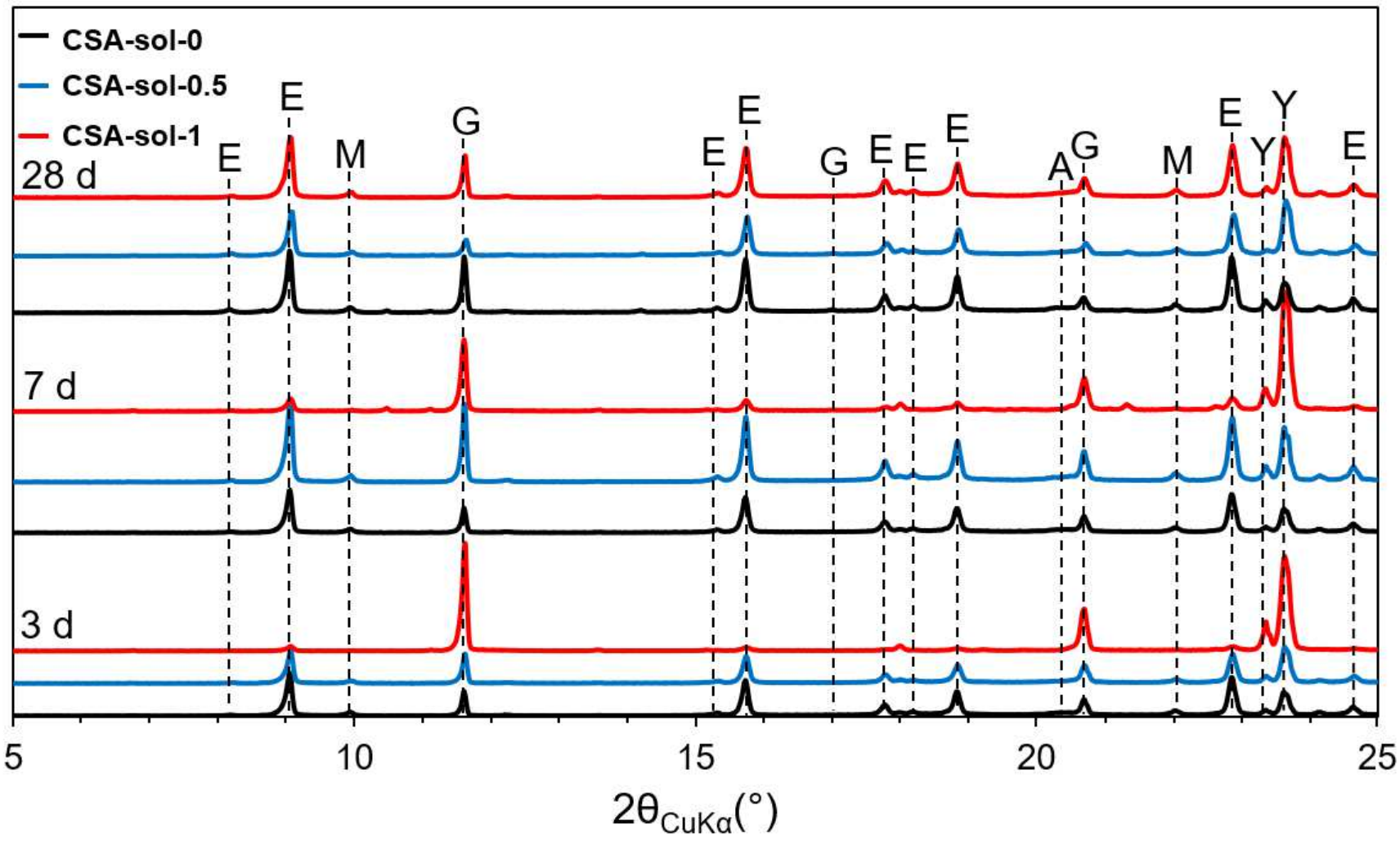


Figure 8 - (a)

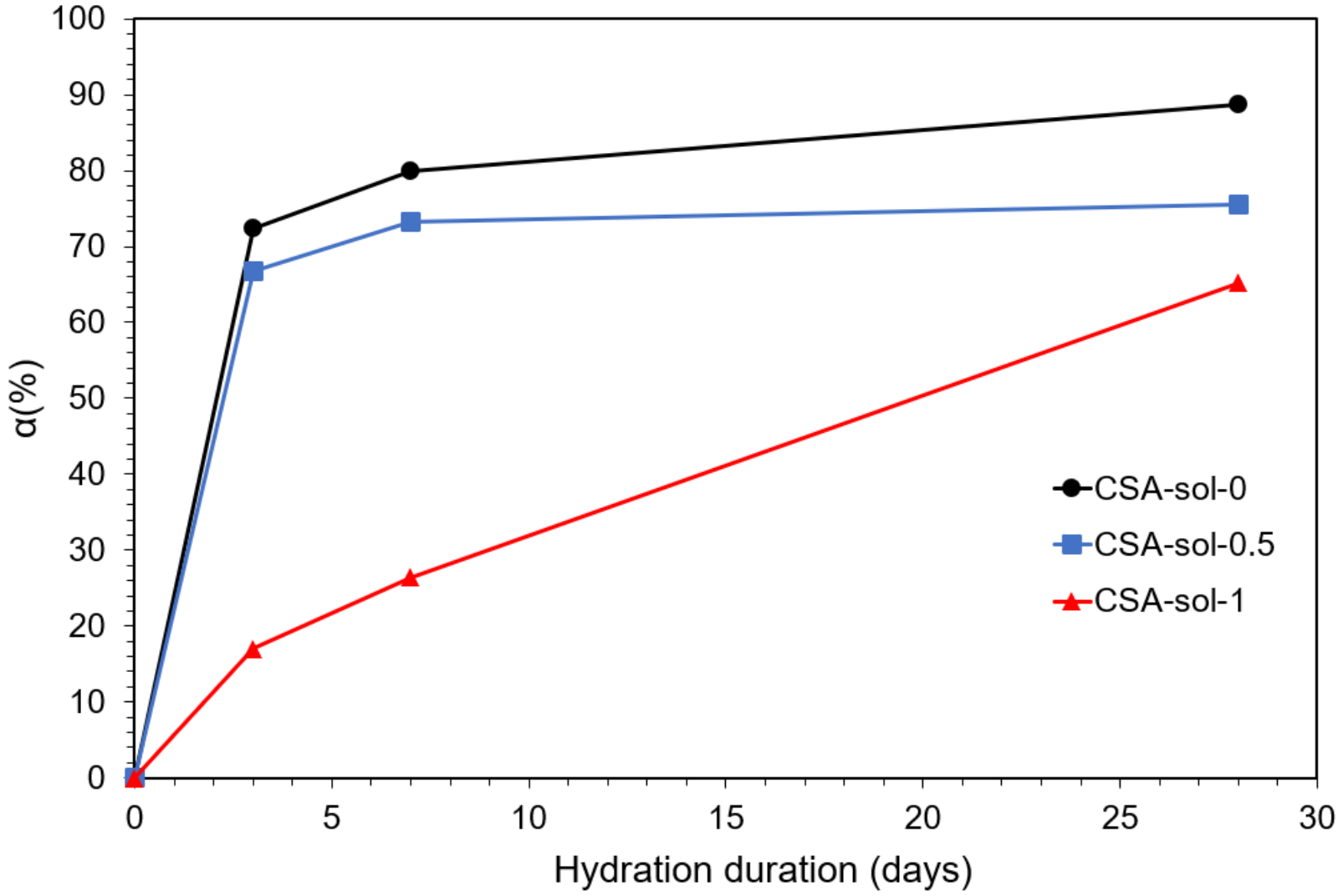

100
90
80
70
60
50
40
30
20
10
0
α(%)
0
5
10
15
20
25
30
Hydration duration (days)
CSA-sol-0
CSA-sol-0.5
CSA-sol-1

Figure 8 - (b)

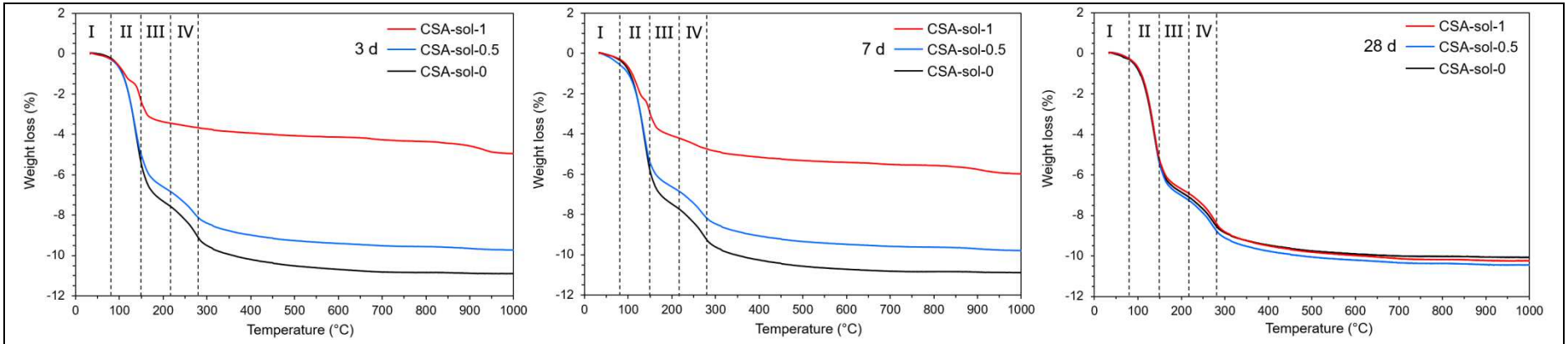

I
II
III
IV
3 d
7 d
28 d
CSA-sol-1
CSA-sol-0.5
CSA-sol-0
Weight loss (%)
Temperature (°C)

Figure 8 - (c)

Table captions

Table 1	Presentation of all prepared samples the corresponding performed characterizations techniques.
Table 2	ICSD collection codes used for XRD-Rietveld quantitative analysis.
Table 3	Physical and chemical characteristics of the ye'elimite powders (Ye-sol and Ye-chem).
Table 4	Zeta potential measurements of the prepared ye'elimite suspensions.
Table 5	Results of Rietveld phase analysis (wt.%) for model cements (CSA-sol) and (CSA-Chem) at different hydration ages. Rietveld agreement factors are also given.
Table 6	Results of Rietveld phase analysis (wt.%) for model cements (CSA-sol-0), (CSA-sol-0.5) and (CSA-sol-1) at different hydration ages. Rietveld agreement factors are also given.

Table 1

	Sample name	Preparation method	Characterizations
For the study of ye'elimite dissolution (W/C = 1000)	Ye-sol	Fig. 2a	IC / SEM †
	Ye-sol-5	Fig. 2b	IC / SEM
	Ye-sol-10	Fig. 2b	IC / SEM
	Ye-chem	Fig. 2a	IC / SEM
For the hydration study of CSA ye'elimite-rich cement (W/C = 2), C = Ye + Gy	CSA-sol-0	Fig. 3-a	XRD-Rietveld analysis TGA-DTG
	CSA-sol-0.5	Fig. 3-b	XRD-Rietveld analysis TGA -DTG
	CSA-sol-1	Fig. 3-b	XRD-Rietveld analysis TGA -DTG
	CSA-chem	Fig. 3-a	XRD-Rietveld analysis TGA -DTG

† IC: continuous ionic conductivity measurement, SEM: scanning electron microscopy, XRD: X-ray diffraction, TGA: thermogravimetric analysis, DTG: Derivative thermogravimetry.

Table 2

Phase name	Formula	ICSD codes	Ref.
Orthorhombic ye'elimite	$C_4A_3\overline{S}$	237892	[31]
Ettringite	$C_6A\overline{S}_3H_{32}$	155395	[32]
Monosulfoaluminate	$C_4A\overline{S}H_{12}$	100138	[33]
Gibbsite	AH_3	6162	[34]
Gypsum	$C\overline{S}H_2$	151692	[35]

Table 3

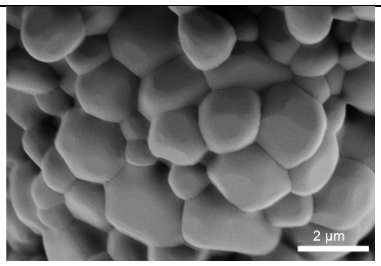
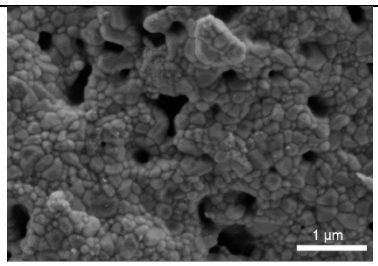
		Ye-sol powder	**Ye-chem powder**
Synthesis method		Solid-state reactions	Sol-gel chemical route
Synthesis protocol details		Ref. [25]	Ref. [39]
Synthesis temperature (°C)		1300	1250
PSD	d10 (µm)	3.1	8.6
	d50 (µm)	14.6	27.1
	d90 (µm)	51.1	68.0
SSA_{BET} (m^2/g)		0.74	2.2
Rietveld analysis	$C_4A_3\bar{S}$ (wt.%)	99.2	98.3
	CA (wt.%)	-	1.7
	CA_2 (wt.%)	0.8	-
Microstructure (SEM)			
Ye'elimite average grain size		2 ±1.2 (µm)	136 ±48 (nm)

Table 4

Ye'elimite suspension	ζ (mV)
Ye-sol-0	7.7 ± 0.3
Ye-sol-5	-0.2 ± 0.1
Ye-sol-10	-10.9 ± 2.8

Table 5

Phase	CSA-sol				CSA-chem			
	t_0	3 d	7 d	28 d	t_0	3 d	7 d	28 d
Ye'elimite $C_4A_3\overline{S}$	63.9	17.6	12.8	7.2	63.9	2.4	1.5	0.7
Gypsum $C\overline{S}H_2$	36.1	9.6	8.6	4.5	36.1	1.9	0.8	0.7
Ettringite $C_6A\overline{S}_3H_{32}$	-	58	65.9	45.0	-	74.1	52.2	83.0
Monosulfo-aluminate $C_4A\overline{S}H_{12}$	-	0.1	0.1	28.5	-	0.2	29.5	0.5
Gibbsite AH_3	-	14.7	12.6	14.8	-	21.4	16.0	15.1
Sum of hydrate amounts	-	72.8	78.6	88.3	-	95.7	97.7	98.6
R_{wp} (%)	-	19.9	18.5	16.8	-	23.1	18.8	21.8
R_{exp} (%)	-	2.8	3.6	2.9	-	2.6	2.7	2.6
GOF	-	7.1	5.1	5.8	-	8.7	6.9	8.3

Table 6

Phase	CSA-sol-0				CSA-sol-0.5				CSA-sol-1			
	t_0	3 d	7 d	28 d	t_0	3 d	7 d	28 d	t_0	3 d	7 d	28 d
Ye'elimite $C_4A_3\overline{S}$	63.9	17.6	12.8	7.2	63.9	21.3	17.1	15.6	63.9	53.0	47.0	22.2
Gypsum $C\overline{S}H_2$	36.1	9.6	8.6	4.5	36.1	13.0	13.1	3.3	36.1	30.5	20.1	10.2
Ettringite $C_6A\overline{S}_3H_{32}$	-	58	65.9	45.0	-	54.2	60.2	39.9	-	8.4	17.1	54.4
Monosulfo-aluminate $C_4A\overline{S}H_{12}$	-	0.1	0.1	28.5	-	0.1	0.1	24.0	-	0.1	9.5	0.2
Gibbsite AH_3	-	14.7	12.6	14.8	-	11.4	9.5	17.2	-	8.0	6.3	13
Sum of hydrate amounts	-	72.8	78.6	88.3	-	65.7	69.8	81.1	-	16.5	32.9	67.6
R_{wp} (%)	-	19.9	18.5	16.8	-	18.1	21.4	15.9	-	21.2	17.2	20.4
R_{exp} (%)	-	2.8	3.6	2.9	-	3.7	2.7	3.0	-	4.0	3.2	2.8
GOF	-	7.1	5.1	5.8	-	4.9	7.8	5.3	-	5.4	5.4	7.2